ACS SENSORS

pubs.acs.org/acssensors

Review

A Review on the Role and Performance of Cellulose Nanomaterials in Sensors

Kelcilene B. R. Teodoro, Rafaela C. Sanfelice, Fernanda L. Migliorini, Adriana Pavinatto, Murilo H. M. Facure, and Daniel S. Correa*

Cite This: *ACS Sens.* 2021, 6, 2473–2496

Read Online

ACCESS | Metrics & More | Article Recommendations

ABSTRACT: Sensors and biosensors play a key role as an analytical tool for the rapid, reliable, and early diagnosis of human diseases. Such devices can also be employed for monitoring environmental pollutants in air and water in an expedited way. More recently, nanomaterials have been proposed as an alternative in sensor fabrication to achieve gains in performance in terms of sensitivity, selectivity, and portability. In this direction, the use of cellulose nanomaterials (CNM), such as cellulose nanofibrils (CNF), cellulose nanocrystals (CNC), and bacterial cellulose (BC), has experienced rapid growth in the fabrication of varied types of sensors. The advantageous properties are related to the supramolecular structures that form the distinct CNM, their biocompatibility, and highly reactive functional groups that enable surface functionalization. The CNM can be applied as hydrogels and xerogels, thin films, nanopapers and other structures interesting for sensor design. Besides, CNM can be combined with other materials (e.g., nanoparticles, enzymes, carbon nanomaterials, etc.) and varied substrates to advanced sensors and biosensors fabrication. This review explores recent advances on CNM and composites applied in the fabrication of optical, electrical, electrochemical, and piezoelectric sensors for detecting analytes ranging from environmental pollutants to human physiological parameters. Emphasis is given to how cellulose nanomaterials can contribute to enhance the performance of varied sensors as well as expand novel sensing applications, which could not be easily achieved using standard materials. Finally, challenges and future trends on the use of cellulose-based materials in sensors and biosensors are also discussed.

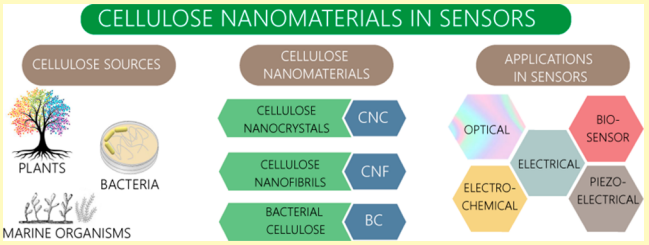

KEYWORDS: *natural polymers, cellulosic materials, optical sensor, piezoelectric sensor, electrical sensor, electrochemical sensor, biosensor, chiral nematic organization, electrode modification, electrospinning*

The investigation and application of sensors and biosensors as an analytical tool for monitoring analytes related to environmental contamination and human diseases have drastically increased in the past years.[1,2] When compared to conventional spectroscopic and chromatographic analytical techniques, sensors and biosensors offer advantages in terms of simplicity of procedures, cheaper reactants, and flexibility for on-site analysis.[3,4] Besides, the detection of various analytes at very low concentrations can be improved by using nano-engineered materials with increased surface area-to-volume ratio and specific functionalities to improve chemical and/or biological recognition. Such a goal is required for the transduction mechanism,[5−8] having a positive impact on the sensitivity, specificity, reproducibility, and portability of varied sensors.[8−10]

Among the myriad materials available for sensor fabrication, recently efforts have been conducted on natural polymers as substrates or even as components of the sensor active layer.[11−14] Such materials can add to sustainability by minimizing the use of nonrenewable and toxic/hazardous components and in some cases can render biocompatibility to the final sensors. This is the case of cellulose, the fundamental skeletal component in the plant kingdom and the most abundant biopolymer on Earth.[15] More specifically, the number of investigations on cellulose nanomaterials (CNM) have experienced a dramatic increase in the last two decades, and the remarkable advances enabled the first industries to produce CNM in commercial large scale.[16] In the past few years, several young companies worldwide have started to bring CNM-based products to the market.[16,17] The remarkable progress in the CNM field is reflected by the large number of publications and patents in this field,[18] including some excellent review papers reporting the use of CNM in

Received: March 4, 2021
Accepted: June 10, 2021
Published: June 29, 2021

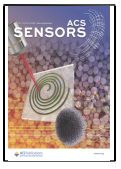

https://doi.org/10.1021/acssensors.1c00473
ACS Sens. 2021, 6, 2473−2496

sensors.[12,19−25] However, there is still room for a critical report on the advantageous use of CNM and their composites applied in sensors and biosensors and how they influence the final devices' performance, which is the aim of the review, as illustrated in Scheme 1.

Scheme 1. Schematic Illustration of CNM and CNM-Based Nanocomposites Applied in the Design of Optical, Electrical, Electrochemical, and Piezoelectric Sensors and Biosensors

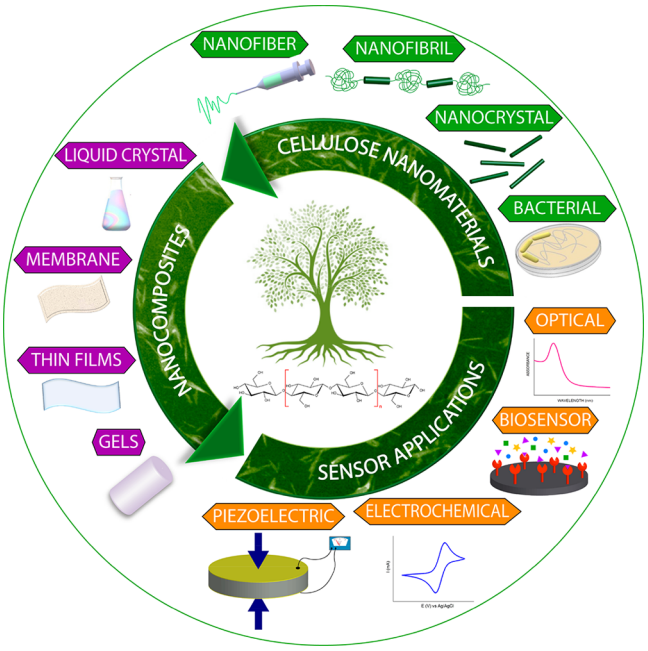

Cellulose: A Brief Introduction. Paper, fabric, and wood are currently the most common materials associated with cellulose; they have been explored since ancient civilizations, over 3500 years ago. Indeed, the first plastics were derived from cellulose in the mid-19th century (cellulose nitrate), and during the depression in the 1930s and World War II, industrial supplies were limited, and so the use of natural materials such as cellulose was again disseminated.[26] However, nowadays cellulose is known as an easily functionalizable polymer with many other industrial applications, such as mechanical reinforcement of composites,[27] a biomedical and pharmaceutical component (excipient, drug delivery, or wound healing dressing material, among others),[28] additive in the food industry,[29] packaging,[30] conductive paper as a component for energy devices,[31] etc. This scenario has inspired cellulose extraction from other sources than conventional wood and cotton, including agricultural residues,[32] bacteria (e.g., *Acetobacter xylium*), marine animals (e.g., tunicates), algae (e.g., *Valonia*), and even amoeba (*Dictyostelium discoideum*).[33]

In plants, polysaccharides represent about 90% of the dry mass of the plant cell wall, composed mainly of cellulose (from 40% to 90%) and fractions of hemicelluloses, pectins, and lignin, whose cellulose percentage vary accordingly to the source.[32] The supramolecular structure of superior plants is illustrated in Figure 1A. The lowest level of hierarchical structure of a cellulosic fiber is the cellulose polymer chain, preceded by the network of intra- and intermolecular interactions between them, assembling individual cellulose molecules into larger units, called elementary fibrils (proto-

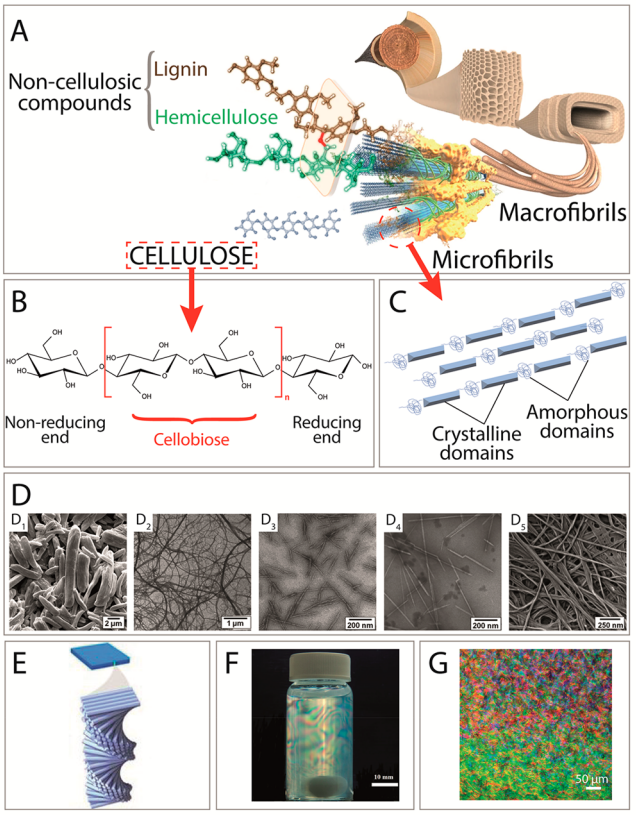

Figure 1. (A) Supramolecular structure of cellulose in a superior vegetal fiber and the organization of its main components. Adapted with permission from ref 36. Copyright 2018 Springer Nature. (B) Representation of a cellulose molecule with the $^4C_1$ chair conformation, pointing out the cellobiose as the repeating unit and the reducing and nonreducing end chains. (C) Representation of cellulosic amorphous and crystalline phases in a microfibril. (D) Micrographies of (D_1) MCC and the different types of CNM: (D_2) CNF, (D_3) wood CNC, (D_4) tunicates CNC, and (D_5) BC. Adapted with permission from ref 37. Copyright 2011 The Royal Society of Chemistry. (E) Cellulose crystallites arranged as a screw-like pack and the helical twist normal to the long axis of the rod. Adapted with permission from ref 38. Copyright 2019 Spring Nature. (F) Iridescent/pearlescent visual aspect between crossed polarizers showing the birefringent domains. Adapted with permission from ref 39. Copyright 2019 John Wiley and Sons. (G) Fingerprint pattern in the chiral nematic phase of a sulfuric acid hydrolyzed CNC aqueous suspension. Adapted with permission from ref 39. Copyright 2019 John Wiley and Sons.

fibrils). The protofibrils, in turn, pack into larger units called microfibrils, whose cross-sectional dimensions usually range from 2 to 20 nm, depending on the cellulose source, while the length is on the micrometer scale.[17] It is important to emphasize that celluloses from different sources may pack themselves in different ways, and such organizations are ruled by the biosynthesis conditions.[34]

Another promising cellulose source is the bacterial cellulose (BC), which displays a chemical and supramolecular structure similar to that of cellulose obtained from plants, being composed of ultrafine cellulose fibrils with a diameter in the range of 80−150 nm.[35] However, unlike plant-based cellulose, BC is free of hemicellulose, pectin, and lignin, which provides a very pure material and well-organized nanofibrillar network structure.[33]

https://doi.org/10.1021/acssensors.1c00473
ACS Sens. 2021, 6, 2473−2496

The isolation of cellulose was first reported by the French Chemist Anselme Payen, in 1838, who named the fibrous material cellulose and defined its molecular formula as $(C_6H_{10}O_5)_n$,[40] as shown in Figure 1B. The cellulose structure comprises linear homopolymer chains, whose physical−chemical properties are overwhelmingly given by the cohesiveness arising from the large amounts of hydroxyl groups available and due to the strong intra- and intermolecular hydrogen bonds. Resulting properties include low water solubility, elevated crystallinity index, and high thermal stability.[41,42] The degree of polymerization (DP) of natural cellulose of various sources is in the range of 1000−30,000, which corresponds to chain lengths of 500−15,000 nm.[35] The manner whereby the cellulose chains are arranged can result in six interconvertible allomorphic forms, identified as cellulose I to cellulose VI, albeit cellulose I presents a thermodynamically metastable structure and can be converted to other allomorphs.[37]

Cellulose functionality can be increased by surface chemical modifications, the strategy of which has been successfully implemented in several studies in order to adapt CNM to their final use. In general, the surface modifications aim to decrease the hydrophilic nature of CNM in order to better disperse in hydrophobic matrices.[43] However, the strategy of chemical modification can also be explored in order to enhance some of the cellulose properties aimed at sensor application.[8,12,44] For instance, controlled reaction conditions can modify the cellulose chains located at the CNM surface by replacing the exposed hydroxyl groups by other chemical groups relevant to the intended application, while preserving the internal CNM structures. Cellulose active sites are the −OH of the C2 and C3 positions, which correspond to secondary alcohols, and the −OH of the C6 position as a primary alcohol. The relative reactivity of these groups follows OH−C6 ≫ OH−C2 > OH−C3.[41] Moreover, CNM can be surface tailored by physical adsorption of functional materials, resulting in hybrid materials, such as CNM−silver nanoparticles and CNM−graphene hybrid materials.[45−47]

Fundamentals of Cellulose Nanomaterials. According to the international organization for standardization (ISO/TS 20477:2017[48]), the term cellulose nanomaterials (or nanocelluloses) comprises materials composed predominantly of cellulose with at least one dimension at the nanoscale, and comprises three categories: bacterial cellulose (BC, also known as microbial cellulose or biocellulose),[42,49,50] cellulose nanofibrils (CNF, also called nano/microfibrillated cellulose),[18,51,52] and cellulose nanocrystals (CNC, also previously referred to as nanocrystalline cellulose and cellulose whiskers).[15,40,53] Morphological aspects of all these CNM, as well as those of commercial microcrystalline cellulose (MCC) and CNC from sea animals (tunicates), can be observed in Figure 1D. CNM are distinct from the commercial MCC, where the latter comprises a fine, white, and odorless crystalline powder extensively applied in pharmaceutical, food, paper, and composite manufacturing.[35] Such products are typically derived from the sulfuric acid treatment of bleached kraft wood fibers or cotton, followed by washing and spray-drying, reagglomerating the smaller cellulosic crystalline domains through hydrogen bonding, which results in particles with minimum dimensions of 1 μm (see Figure 1D$_1$).[54] MCC has been used as the starting material of several pioneering studies in NC isolation.[55−58]

CNM can be synthesized by using bottom-up and top-down approaches.[17] Regarding the top-down approach, two typical classes of CNM can be obtained by deconstructing the hierarchical structure of a cellulosic microfibril, which is illustrated in Figure 1A: CNF through mechanical processes, and CNC through chemical/enzymatic hydrolysis. Specifically, CNF are generated from top-down mechanical procedures applied to microfibrils (pretreated or not), in which high shear and impact forces are applied to vegetal fibers, leading to mechanical cleavage along the longitudinal direction of the cellulose microfibrillar structure.[59] As a result, part of noncellulosic compounds are eliminated, but considering that no corrosive reactant is added, the cellulosic amorphous phase remains, yielding more flexible and longer nanostructures (length >1 μm, cross section ca. 5 nm), constituted by alternate association of highly ordered and amorphous cellulosic domains.[60] The morphological features of CNF easily induce entanglement at extremely low concentrations, which opens a wide window of applications for paper, membranes, hydrogel, and xerogel.[61]

Additionally, artificial cellulose nanofibers can be engineered by applying versatile top-down spinning techniques (electro-, wet , dry, and solution blow spinning) with distinct morphologies, dimensions, and functionalities.[62−64] These methods consist basically of the ejection of a droplet of the polymer solution/melt due to driving forces (e.g., electrical, gas pressurized, and centrifugal forces) followed by the rapid solidification by precipitation or solvent evaporation.[65,66] The spun fibers network is collected as a nanofibrous mat, rich in pores and channels, facilitating their configuration as a high-surface-area membrane, nanopaper, aerogels, and thin films that can also be directly deposited onto the electrode surfaces for sensor application.[67,68] Due to the insolubility of cellulose in water and in most organic solvents, caused by its supramolecular structure, researchers have also worked with cellulose derivatives. In general, a cellulosic polymer structure can be solubilized by solvents not suitable to spinning techniques, as LiCl in DMA (DMA/LiCl), tetrabutylammonium fluoride trihydrate in DMSO (DMSO/TBAF), or cuprammonium hydroxide.[40] Cellulose derivatives include cellulose acetate, hydroxypropyl cellulose, hydroxypropyl methylcellulose, and ethyl-cyanoethyl cellulose, which can be dissolved in volatile solvents suitable for most of the spinning techniques. Cellulose acetate, in particular, has been electrospun under a wide variety of conditions and subsequently deacetylated to form cellulose nanofibers or functionalized with other side groups.[68,69]

Owing to the semicrystalline nature of a microfibril (as illustrated in Figure 1C), controlled acid or enzymatic hydrolysis conditions lead to amorphous domain removal and isolation of very thin single crystals called CNC. Hydrolysis kinetics is faster for noncrystalline regions than for crystalline domains, as it is the hydrolytic cleavage of glycosidic linkages promoted by the penetration of the hydronium ions into noncrystalline regions.[70] The conventional use of sulfuric acid in hydrolysis promotes the esterification of the CNC surface hydroxyl groups, leading to a high number of negatively charged sulfate groups on the surface of CNC, which limits the agglomeration and flocculation of CNC in aqueous medium.[50,71] Needle-like CNC structures are thereby obtained whose diameters vary from 5 to 20 nm and length from 100 nm to 1−2 μm.[37,72] CNC are traditionally applied as mechanical reinforcement to

https://doi.org/10.1021/acssensors.1c00473
ACS Sens. 2021, 6, 2473−2496

nanocomposite materials, but more recently, CNC have been explored in diverse applications, including sensors and optoelectronic devices.[17,22,73−75]

BC is considered a bottom-up approach employed to produce CNM with the aid of microorganisms such as *Gluconacetobacter xylinus, Bacillus megaterium, grobacterium, Alcaligenes, Pseudomonas, Rhizobium, or Sarcina*, where the first presents the highest capacity of cellulose production.[42,76,77] A cellulosic 3D network is collected as planar gel-like films (fleeces/pellicles) with the same shape and dimensions of cultivation reservoir or can be brought into a complex 3D shape by the use of templates.[17] Its gel nature effortlessly moves the BC toward hydrogel and xerogel configuration for several applications, mainly in the biomedical area. Especially due to its purity and ideal biocompatibility, BC shows an unprecedented potential as a substrate for wearable sensors.[78−80] It is important to mention that BC can also be applied as a starting material for CNC production.[81]

It is also important to emphasize that the final properties and features of BC, CNF, and CNC are highly affected by the cellulose source and experimental conditions. Thus, pretreatments are usually required to purify and homogenize the starting material, removing noncellulosic materials, namely, lignin and hemicelluloses for plants, the bacteria and the culture media for BC, and protein matrix for tunicates.[82−84] The purification of the starting material is important to guarantee that the functional groups of cellulose are more exposed for surface interaction with other materials. Besides, purified cellulose materials have more uniform properties, higher Young's modulus[85,86] (important for wearable and nonwearable flexible sensors), dimensional stability[87,88] (for piezoelectric sensors), and transparency[89,90] (also required for some types of sensors and electronic devices).[37,43,71]

Cellulose Nanomaterials in Sensors: Structure−Properties−Application. CNM possess many interesting properties for the development of chemical sensors, including molecular polarization, electrostatic interactions, and switchable hydrogen bonds.[20] Besides, CNM anisotropy attained by controlled self-assembly CNC suspensions can yield optical birefringence and bright iridescent materials for colorimetric sensors and biosensors. Specifically, well-dispersed CNC separate into a lower chiral nematic liquid crystalline phase (a state of matter with characteristics between a liquid and a solid) and an upper isotropic phase above a critical concentration of ca. 4.5 wt %.[43] According to ref 37, the crystallites arrange themselves in a helical twist down the long axis normal to the rod, at an angle which intertwines the "threads" (Figure 1E). In this way, the CNC stacked planes align along a perpendicular axis, with each plane rotating at a phase angle, depending on concentration. Thus, this alignment can result in optical band-gaps providing iridescent/pearlescent visual aspect between crossed polarizers (displayed in Figure 1F), due to the birefringence of individual domains, typically producing fingerprint patterns as shown in Figure 1G. This CNC intrinsic feature has been explored in liquid-phase and solid-phase sensors, in which the optically active arrangement is retained in a polymer matrix or in a CNM film.[91] The chiral nematic organization of CNC is always left-handed, and then the CNC films selectively reflect left-handed light, showing up colorful when the helical pitch (P) is on the order of magnitude of the visible-light wavelength, since P can be controlled through physical condition changes, and thus, it is relatively straightforward to modulate the color of the film.[15]

Furthermore, the interest in fabricating low-cost, self-standing, flexible, biodegradable, and high-surface-area sensing platforms has promoted the application of CNM as substrates and biotemplates/scaffolds for hosting functional materials through varied approaches. CNM can also be employed as flexible and transparent films and coatings in optical and electronic devices. Films exclusively constituted by CNM are so-called nanopaper, which can show optical transparency if the cellulose nanofibers are densely packed and the interstices between the fibers are small enough to avoid light scattering.[15] In addition, the chemical composition and structure of foams, aerogels, and biofilms based on CNM can perform important roles in sensing and biosensing.[92−94]

An interesting growing trend is the use of paper and nanopaper as substrates for electrode fabrication, allowing the substitution of traditional glass- or plastic-based material by cheaper and disposable materials. In this direction, standard paper has received great attention for application in the printed sensors field seeking improvements offered by (i) easy load and delivery of reagents in the 3D cellulose network; (ii) capability to perform the analysis using small volumes of samples, largely reducing reagents and sample quantities; (iii) pores and channels of cellulosic substrate developing an important role for sample treatment, avoiding the interference of particulates present in the sample, which keeps them entrapped at the substrate surface enabling the analyte to flow toward the electrode surface; (iv) microfluidics without the need of micropumps for flow generation, as well as circumventing bubble formation (which is a common issue in classical microfluidic systems).[95] Once it was observed that thin films produced with CNM presented properties different from those of common paper, a new field of investigation was developed toward flexible optoelectronic devices. A milestone study was reported by Revol et al.,[96,97] who obtained nanopaper by drying a CNC aqueous suspension through simple evaporation.[97,98] Afterward, CNF extracted from vegetal and animal sources was employed in nanopaper fabrication[99−101] and also the BC, which was explored by Morales-Narvaez and co-workers[102] in configuring several nanopaper-based optical sensing platforms.

For BC, the advantageous properties for sensing application are based on its similarity to the extracellular matrix of the skin, including in fiber diameter and porosity, and a high degree of purity. This mimicking reflects preferential binding of biomolecules with the BC substrate instead of the electrodic surface.[78] Besides, proper chemical modification of BC can lead to immobilization of biomolecules by covalent linkage, which prevents the leaching during the sensing analysis,[78] enhancing the sensitivity and reproducibility of biosensors. In this direction, BC has been used for biosensing biomarkers present in body fluids related to important diseases, as α-amylase,[103] Parkinson's disease biomarker,[104] metal ions,[105] and early cancer screening.[106]

In addition, there are a plethora of studies reporting the immobilization of biomolecules on CNM.[8,78,95,106,107] The high content of −OH groups available in CNM allows their functionalization, enabling adsorption of varied molecules. However, oxidized or carboxylated CNM are preferred for the immobilization of biomolecules in biosensors, in order to promote amide linkage between amide groups of proteins and nucleic acids, and carboxyl groups grafted onto cellulose molecules.[108] The immobilization by covalent bond is preferred, in contrast to physical adsorption, because the

https://doi.org/10.1021/acssensors.1c00473
ACS Sens. 2021, 6, 2473−2496

Table 1. Recent Papers Reporting the Application of CNM in Optical Sensor Devices

Analytes or properties under investigation	Role of CNM in the analyte detection	Materials employed in the sensor [ref]
Environmental humidity/ water	Swelling process enlarging the helical pitch of the chiral nematic structure	CNC/polyacrylamide composites[132]
		Chiral nematic CNC/glycerol[133,134]
		CNC[135]
		CNC/poly(ethylene) glycol[136]
		CNM paper/waterborne polyurethane[137]
Mechanical stress	Reduction in the helical pitch	Chiral nematic CNC/elastomer composites[138]
		Chiral nematic CNC plasticized with glycerol[134]
		CNC-polyvinyl alcohol-glucose[139]
		CNC chiral nematic liquid crystals[140]
Vapor sensing	Increase of the distance between the film layers owing to the affinity between gas molecules and CNM	Colloidal CNC[128]
		Iridescent chiral nematic CNC/PVP nanocomposites[141]
		Oxidized CNC[142]
		Cellulose/PMMA[143]
		Cu(II)-doped CNC[144]
		CNC functionalized with amine groups[91]
Biomolecules	Analyte immobilization by electrostatic interaction	Peptide-CNM[145]
		BC and curcumin (paper-based)[146]
		CNC and carbon quantum dots[147]
Temperature	Relationship between surface structure and temperature	CNC−4′-(hexyloxy)-4-biphenylcarbonitrile[148]
		CNC-assisted carbon dots grafted $SrAl_2O_4$, Eu^{2+}, Dy^{3+} phosphors[111]
Metals	Chelation of metal	BC paper with curcumin[149]
		AuNPs supported by CNC[110]
H_2O_2	Catalytic deposition of AgNPs	CNC and AgNPs[47]
TNT	SERS detection through the Meisenheimer complex formed by the interaction between AuNT@AgNCs and TNT	Au nanorods/Ag CNM[150]
Fungicide and pesticide malachite green	Amplification of SERS signals caused by interaction between AgNPs and the analyte	AgNPs/CNC[151]

physical−chemical changes in environmental conditions can disturb the system.[109] Besides, CNM surfaces show low adhesion of nontarget interfering molecules present in physiological fluids.[108]

Electrical and electrochemical sensors have also taken advantage of CNM-based materials for designing sensors. For instance, the design of conductive CNM-based nanocomposites can be achieved by efficiently combining CNM to plasmonic NPs,[75,110] photoluminescent NPs,[102,111] inorganic NPs,[112] carbon-based nanomaterials,[45,113] conductive nanomaterials,[107,114] and biological compounds.[58,115,116] The CNM surface functionalization can be achieved through physical adsorption of conductive materials using solution/vapor deposition, sputter coating, layer-by-layer and other methods, as well as by in situ polymerization. Additionally, CNM have also been employed in the synthesis of graphene and metal nanoparticles by taking advantages of the CNM functional groups and high specific surface area. Such a combination of properties allows the production of well-dispersed metallic nanoparticles without using conventional toxic and expensive reactants (e.g., hydrazine and borohydride).[45,46,117,118]

Piezoelectricity is another interesting property arising from the CNM structure suitable for the design of piezoelectric sensors. In piezoelectric materials, an electric charge is generated as result of the application of mechanical stress (direct effect) or, conversely, a mechanical strain the material experiences under an the application of an electric field.[119,120] The piezoelectricity in wood, the discovery of which dates back to 1955,[121,122] arises from the oriented asymmetric arrangement of cellulose crystals.[123] The hydrogen bonds in the cellulose structure contribute to the formation of a dipolar orientation and lead to a permanent polarization, giving rise to the piezoelectric effect, which is related to changes in polarization density and the manifestation of dipole moments.[22,124,125] The shear piezoelectricity in cellulose is comparable to that in quartz crystal[125] and has enabled many applications in sensors, as illustrated in the next sections.

ROLE AND PERFORMANCE OF CELLULOSE NANOMATERIALS IN SENSORS

Cellulose Nanomaterials in Optical Sensors. Optical sensors can detect changes in the materials' optical properties, like color, absorbance, fluorescence, reflectance, and refractive index to monitor different analytes.[20,126−131] This section will survey recent representative studies of CNM applied to optical sensors using techniques such as colorimetry, fluorescence, absorbance, and surface-enhanced Raman scattering (SERS), as summarized in Table 1. It is possible to note that the chiral nematic properties of CNC have been widely employed in optical sensors, and several types of materials can decorate CNM for modulating the sensor response for a given application.

As previously mentioned, under certain conditions, CNM can form a liquid crystal phase, which is promising for the preparation of photonic nanomaterials, mainly because they combine biocompatibility with self-assembly behavior, producing chiral nematic superstructures with interesting optical properties.[152] The structure of CNM chiral nematic liquid crystals observed in suspensions can be preserved in solid films, providing stable platforms with a helical structure and bright iridescent color. Because of the hydrophilicity, when these

https://doi.org/10.1021/acssensors.1c00473
ACS Sens. 2021, 6, 2473−2496

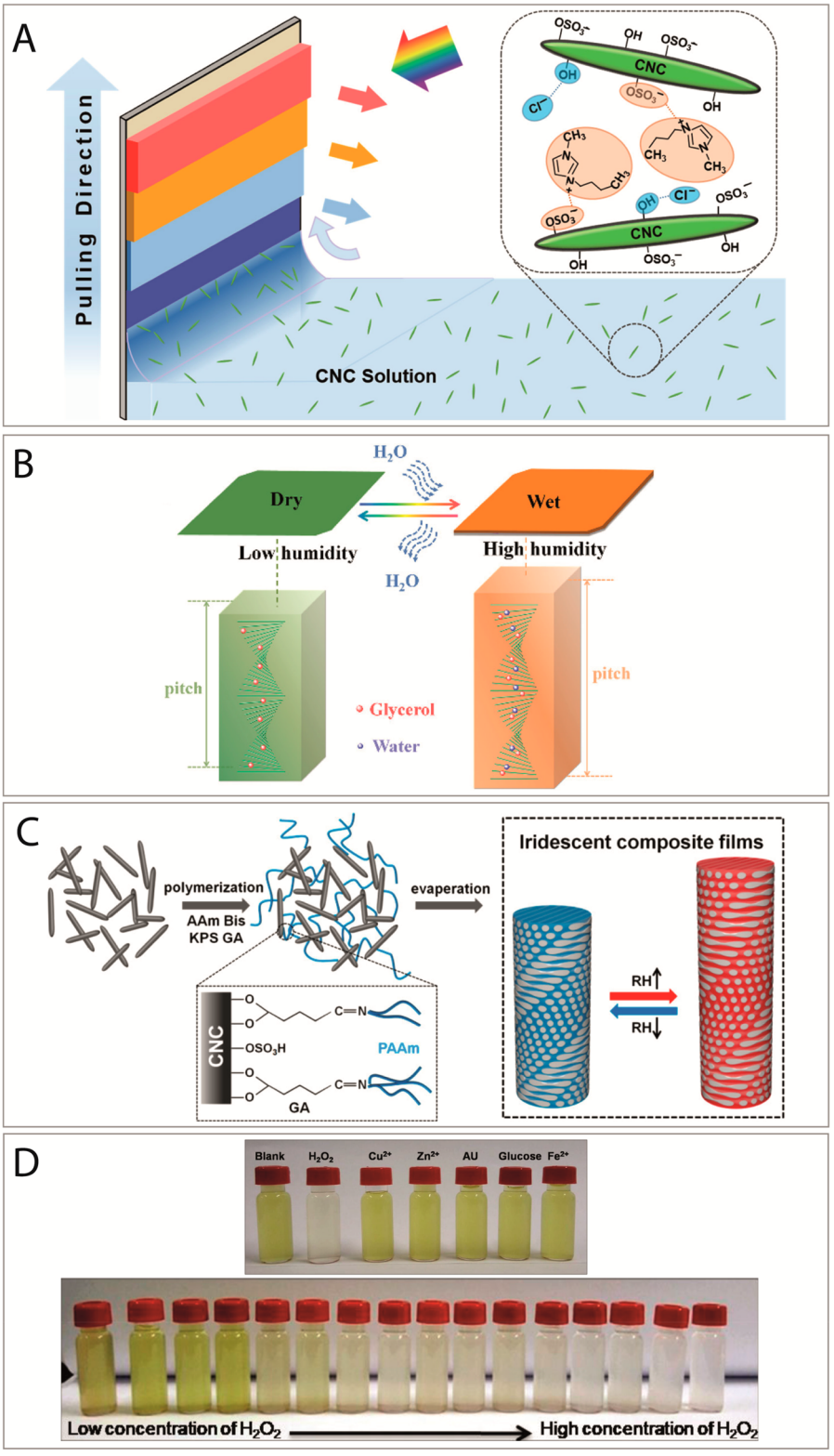

Figure 2. (A) CNC-based color sensor with the incorporation of 1-butyl-3-methylimidazolium. Different film thicknesses, due to the change in the traction speed during assembly, resulted in different colors. Reprinted (adapted) with permission from ref 91. Copyright (2018) American Chemical Society. (B) Schematic mechanism for the reversible humidity-responsive structural color change of CNC-based films. Reprinted (adapted) with permission from ref 134. Copyright (2018) American Chemical Society. (C) Illustration of CNC/polyacrylamide synthesis and the change in the iridescent composite films due to humidity increase. Reprinted (adapted) with permission from ref 132. Copyright (2017) American Chemical Society. (D) Photographs of AgNP/CNC solutions exposed to various concentrations of H_2O_2, where the catalytic decomposition of AgNP in the presence of H_2O_2 caused a decrease in the AgNP absorption band at 410 nm. Reprinted (adapted) with permission from ref 47. Copyrigth (2019) Elsevier.

https://doi.org/10.1021/acssensors.1c00473
ACS Sens. 2021, 6, 2473−2496

films are exposed to environments with high relative humidity, they swell due to the water absorption, causing changes in the CNM pitch. Specifically, when the films swell, the chiral nematic step increases linearly with an increase of the interspaces between the CNM pseudoplanes, causing color changes. The color change is smaller at low humidity values, since CNM have a limited capacity to capture moisture.[20] Thanks to this characteristic, the CNM chiral nematic films have been widely used in humidity sensors.[135,136,153,154] In this direction, Bumbudsanpharoke et al. recently reported two studies involving humidity detection using colorimetric sensors based on CNM chiral nematic liquid crystals.[135,154] In the first study,[135] the sensor was developed by adding NaCl to the CNM suspension, yielding a pink-colored film. As the material absorbs moisture, the pink color is shifted 160 nm toward longer wavelengths, visually changing the film color to bluish. The developed optical sensor could monitor humidity in a precise and reversible way, with potential application in smart packaging of products that suffer deterioration when exposed to humidity. The same principle of detection using chiral nematic liquid crystals can be used for sensing volatile organic compounds (VOC). The fixing of VOCs in the film induces swelling of the cellulose-based platform, altering the cholesteric pitch, similarly to what happens with the absorption of humidity.[155] In the work by Shidong et al.,[144] a gaseous ammonia sensor based on CNC chiral nematic films doped with copper(II) was developed. The presence of positively charged copper ions chelated negatively charged CNC and red-shifted the film absorbance by more than 50 nm. The developed platform was sensitive to ammonia gas, since the gas molecules were allocated in the nematic layers of CNC, binding to chelated copper ions, yielding to a redshift in the reflective wavelength as well as a visible colorimetric transition. The authors also developed a kinetic model that quantitatively related the effects of ammonia gas kinetic detection to the change in the reflective wavelength.

The modifier and processing steps employed in the fabrication of films can promote characteristic color changes suitable to be employed in the detection of specific analytes for varied application. For instance, in the work of Song et al.,[91] CNC were used to form a solid substrate displaying different color patterns without adding chemical pigments, which was achieved by selecting film thickness. This parameter was controlled by adjustments in the film assembly process and the addition of 1-butyl-3-methylimidazolium, as shown in Figure 2A. These films were functionalized with amine groups to obtain a low-cost and biocompatible colorimetric sensor capable of changing color in the presence of formaldehyde or propanal gases without interference from other molecules. The detection limit achieved was less than 0.5 ppm, and for observations with the naked eye, this value increased to 7.3 ppm. Similarly, other works have employed CNM as a protagonist in the fabrication of colorimetric films by different techniques using other molecules to functionalize substrates for varied analytes, such as copper doped CNM for ammonia gas sensing,[144] organic solvent detection using a nanocomposite containing CNC and polyvinylpyrrolidone,[141] introduction of small plasticizer molecules onto CNC to improve the humidity sensing,[134] and humidity sensing using a nanocomposite based on CNC and polyacrylamide,[132] among others.[133,136,142,145] The significant advantages of these colorimetric sensing platforms include their biocompatibility, low cost, and the possibility of forming hybrid compounds with different classes of molecules or ions.

The color modification process of CNC-based films can be better understood by observing Figure 2B[134] and C.[132] CNM can exhibit the properties of chiral nematic liquid crystals and therefore can reveal distinct colors without the use of chromophores. Such materials can behave like a self-organizing, one-dimensional chiral photonic crystal, whose axis rotates in the plane around a perpendicular helix, as demonstrated in Figure 1E. As a result, a periodic variation in the refractive index leads the material to behave like a circularly polarized incident light filter. When the functionalized film absorbs vapors, it swells, and the chiral nematic structure step is expanded. Then, the expanded film will reflect light with greater bandwidth than single-pitch films without expansion, changing the material reflectance and color. Additionally, the variation in the material pitch can occur reversibly or irreversibly, depending on the type of analyte.[153]

Due to its selectivity and sensitivity, SERS is considered a powerful technique for biomolecule detection. In this case, CNM can be used as flexible platform with multilayer and 3D nanonetworks for the immobilization of metallic nanoparticles, minimizing agglomeration and aggregation effects. Thus, the role of CNM can be used not only as a sensing layer but also as a flexible, stabilizing support that allows the uniform distribution of nanoparticles on its surface.[150,151,156,157] For instance, in the study reported by Nabeela et al.,[158] the authors investigated the role of CNF in increasing the SERS signal in the detection of organophosphate pesticide methyl parathion. Plasmonic silver nanoconstructs obtained using CNF were able to produce sensors with sensitivity higher than that obtained with neat silver nanoparticles. This behavior was ascribed to the presence of the CNF, which enabled a high density of hotspots provided by the local enrichment of analytes driven by the nanocellulose-silver after drying. Other interesting works using cellulose-based platforms for SERS devices can be found in the literature.[159−161] For instance, Wu et al.[150] reported the use of nanocellulose in the detection of TNT. The sensor platform was composed of a three-dimensional (3D) dispositive containing AuNR@AgNCs on bacterial cellulose aerogels, which could detect 2,4,6-trinitrotoluene (TNT) through SERS analyses. The detection limit for TNT obtained in this work was 8×10^{-12} g/L, and the improvement factor of the SERS signal was high, up to 1.87×10^{8}.

Although CNM-based sensors can present advantageous properties, in some cases the detection is achieved with low selectivity, which can be tackled using dopants in the matrix.[20,148] Ruiz-Palomero et al.[162] reported a fluorimetric sensor based on sulfur, quantum dots of graphene encoded with nitrogen immersed in nanocellulosic hydrogels, which was applied in the detection of the laccase enzyme. The presence of the nanocellulose hydrogel promoted the increase of the fluorescence signal of graphene quantum dots through the self-quenching process. In addition, it stabilized the fluorescence signal, which caused a rise in the sensitivity to laccase. Another interesting property of CNM is its capability to stabilize metallic nanoparticles in the solution,[110,163,164] enabling the composite material to be used in the design of sensing platforms for monitoring varied analytes. For instance, Teodoro et al. developed a colorimetric sensor based on CNC/AgNP hybrid material displaying high sensitivity (detection limits of 0.014 μM) and selectivity toward H_2O_2 detection in water and milk matrices. The mechanism of

https://doi.org/10.1021/acssensors.1c00473
ACS Sens. 2021, 6, 2473−2496

Table 2. Examples of CNM-Based Electrical and Electrochemical (Bio)Sensors for the Detection of Varied Analytes

materials	analyte	detection method	LOD/linear range	ref
Screen-printed carbon electrodes on microbial CNM	Cd^{2+}	DPV	1.01 μM	80
	Pb^{2+}		0.43 μM	
	uric acid		1.8 μM	
	17β-estradiol		0.58 μM	
PA6/CNC:rGO hybrid platform	Hg^{2+}	DPV	0.52/2.5−200 μM	45
Nanocomposites based on electrospun nanofibers modified with CNC:AgNPs, CNC:AuNPs, and CNC:rGO	isoborneol	electrical	25 ng L^{-1}[a]/25−100 ng L^{-1}	189
Cellulose-Modified Pencil Graphite Electrode	herbicide atrazine	SWV	0.008/5−320 ng mL^{-1}	190
methyl cellulose (MC) buffer layers and pentacene	NO_2	electrical	1 ppm	191
TEMPO-nanocrystalline cellulose/PNA[a]/rGO	*Mycobacterium tuberculosis*	DPV	3.14×10^{-14}/1×10^{-8}−10^{-13} M	192
Silylated Graphene oxide−grafted-chemically modified nanocellulose	cholesterol	DPV	7.4 μM/5.18−25.9 μM	193
Nanocrystalline cellulose-CTAB[b]/Tyr[c]/CdS quantum dots	phenol	DPV	0.082 μM/5.0−40.0 μM	194
	cathecol		0.125 μM/1.0−25.0 μM	
	o-cresol		0.007 μM/2.0−10.0 μM	
	4-chlorophenol		0.021 μM/5.0−25.0 μM	
TEMPO oxidized-cellulose nanocrystals/GOx[d]	glucose	amperometry	0.004 mM/0.1−2 mM	195
Nanocellulose/Graphene oxide-Pt-nanocauliflower/GOx[e]	glucose	amperometry	0.08 μM/0−500 μM	196
Nanocellulose/Graphene oxide- Pt-nanocauliflower/RNA aptamer for *E. coli* detection	*E. coli* O157:H7		4 CFU[f] mL^{-1}/ 4−105 CFU/mL	
Bacterial cellulose-Au nanoparticles/laccase	hydroquinone	DPV	5.71 nM/30−100 nM	197
Cellulose nanocrystal/polypyrrole/GOx	glucose	DPV	50 μM/1.0−20.0 mM	107
Fibers (TCNF[g]/CNT[h])	NO_2	electrical	0.5% to 0.125 ppm	198

[a]PNA: peptide nuclide acid. [b]CTAB: cetyl trimethyl ammonium bromide. [c]Tyr: tyrosinase. [d]GOx: glucose oxidase. [e]Pt: platinum. [f]CFU: colony-forming unit. [g]TCNF: nanocellulose extracted from tunicate. [h]CNT: carbon nanotube.

detection was based on the catalytic decomposition of silver nanoparticles (AgNP) in the presence of H_2O_2, causing a decrease in the AgNP absorption band at 410 nm as the H_2O_2 concentration was increased. The solution color changes were observable by the naked eye, according to Figure 2D, without the interference of some common interferents, such as Cu^{2+}, Zn^{2+}, Au^{+}, glucose, and Fe^{2+}, proving the sensor was selective. The sensor performance was associated with the dispersion and stabilization of AgNP onto CNC surface, given by the interactions during the synthesis of silver ions and negatively charged groups (hydroxyl and sulfate) present on the CNC surface. Other metallic materials can also be used to decorate CNM to obtain colorimetric sensors, such as copper for ammonia detection,[144] AgNP for the monitoring of water pollution,[156] and AuNP for monitoring cadmium.[110] Collins et al.[165] described CNM surface modification using the cobalt-(II)-bis-terpyridine complex to prepare colorimetric cyanide sensors. The attached cobalt-based complex exhibited red-orange color in aqueous solution, and the color disappeared in the presence of cyanide ions.

A combination of metals can be an interesting alternative to decorate CNM and expand their application in colorimetric sensors. Such an alternative was reported by Nwosu et al.,[166] who developed a hybrid material composed of CNM-Ag-Cu for the colorimetric detection of urea in solution. The authors obtained a detection limit around 0.8 ppm and selectivity toward other analytes commonly found in human urine. Besides, the reproducibility, evaluated by three consecutive measurements, resulted in a relative standard deviation (RSD) of 2.61%.

Dyes such as rhodamines have also been widely used in synergy with CNM to prepare opto-chemical sensors, due to their remarkable absorbance and fluorescence properties. For instance, rhodamine can form a complex in the presence of some ions, such as Hg^{+2}[167] and Cu^{2+},[168,169] leading to changes in color observable by the naked eye, which makes these materials widely used in colorimetric sensors for metal ions. In such cases, CNM can act as a scaffold for rhodamine immobilization, usually by grafting rhodamine derivates and cellulose. Besides, the use of CNM with rhodamine is interesting due to the biocompatibility of these materials, since rhodamine is extensively applied in the bioimaging and detection of analytes in a biological system.[167]

Since CNM can be modified with fluorescent dyes, the final conjugated system can be applied in the monitoring of some analytes capable of interacting with the modified CNM. In this direction, Xiong et al.[170] reported the use of fluorescent carbon quantum dots (CQDs) for decorating the surface of CNM chiral structures. The chiral organization of the needle-like CNC allowed the self-organization of the CQDs, avoiding particle aggregation. As a consequence, it was possible to obtain highly organized and homogeneous films whose flexibility and characteristic fluorescent fingerprint signature were suitable for designing luminescence-based optical sensors. Other interesting works developed using CQD for the preparation of fluorescent platforms based on CNM can be found elsewhere.[111,147,171]

CNM can also be used in optical sensors as the substrate for fixing the sensor active layer. As a substrate, cellulose nanopaper comprises an internal network structure formed by several layers of cellulose fibers. For being highly flexible, light, cheap, and biodegradable, paper is advantageous compared to other substrates, such as glass and plastic.[139,172,173] In the work by Faham et al.,[149] an analytical device based on cellulose nanopaper was produced through the incorporation of curcumin by laser printing technology. The biocompatible and biodegradable platform was used for monitoring Fe(III) and deferoxamine (DFO) as an iron-

https://doi.org/10.1021/acssensors.1c00473
ACS Sens. 2021, 6, 2473−2496

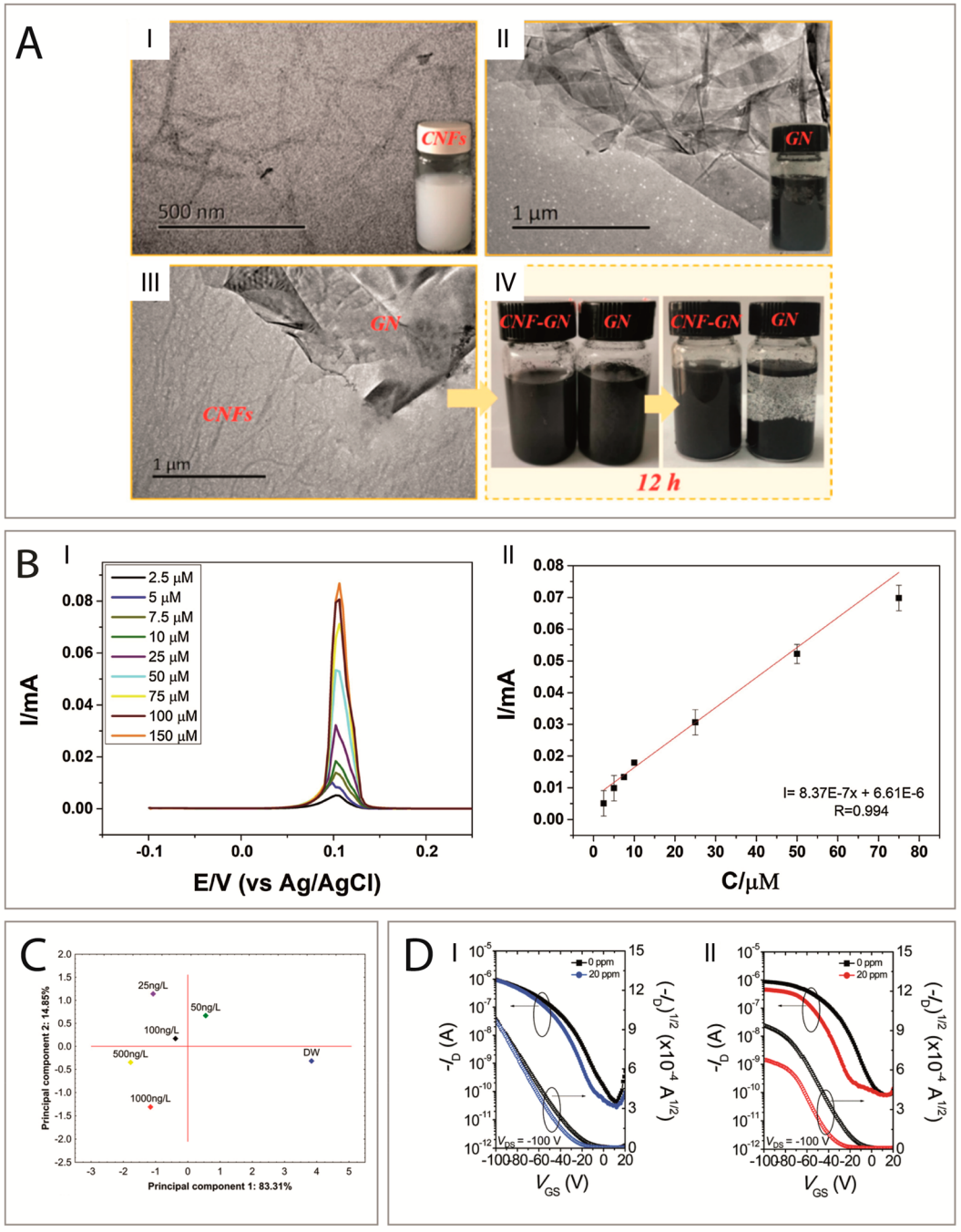

Figure 3. (A) Transmission electron microscope (TEM) images of CNF (I), GN (II), and GN-CNF nanocomplexes (III); (IV) macroscopic pictures of pure GN and GN-CNF dispersions after a 12 h rest. Reprinted with permission from ref 203. Copyright 2019 MDPI. (B) (I) DPV curves for different concentrations of Hg(II) using PA6/CNC:rGO hybrid platform, in 0.1 mol L^{-1} acetate buffer, and (II) the linear relationship between the peak current versus Hg(II) concentrations. Reprinted with permission from ref 189. Copyright 2019 Elsevier. (C) PCA plots for the electrical capacitance responses (experimental data collected with the electronic tongue) at 1 kHz for the analysis of different Isoborneol solutions and distilled water (DW). Reprinted with permission from ref 189. Copyright 2019 MDPI. (D) Transfer characteristics of the pentacene OFET-based sensors (I) without and (II) with MC toward 20 ppm of NH_3 gas flow. Reprinted with permission from ref 191. Copyright 2019 Royal Society of Chemistry.

chelator in biological fluids such as blood, saliva, and urine. In the presence of Fe(III), the color intensity of the CNM-based paper with curcumin decreased due to the formation of a complex between iron and curcumin. This sensor showed high selectivity compared to the response of other interferents present in the human blood (limit of detection around 7.5 nM for Fe(III) and 8.0 nM for DFO), such as creatinine, uric acid, and various metallic ions. The detection limit toward iron was around 7.8 nM, and DFO was around 8.2 nM.

Cellulose Nanomaterials in Electrical and Electrochemical Sensors. Electrical and electrochemical sensors have been successfully employed for the efficient detection of varied analytes. What differentiates one from another is the way the detection is carried out. Generally, electrical sensors

https://doi.org/10.1021/acssensors.1c00473
ACS Sens. 2021, 6, 2473−2496

detect variations in electrical properties, such as an increase/decrease in electrical current or even a change in electrical voltage,[174] whereas the electrochemical sensor converts the effect of the analyte−electrode interaction, which is due to a process of oxidation or reduction, in an electrical signal.[175,176] Both techniques have many advantages, such as, for example, high sensitivity and selectivity, simplicity, moderate cost, and portability.[177,178]

A key feature for both techniques is the choice of material to be deposited onto the electrode surface, since this material will be directly related to the surface area of the electrode, as well as to the sensitivity, specificity, and detection limits of the proposed sensor.[179] Thus, a suitable strategy to improve the sensor performance in terms of sensitivity, specificity, and detection limit is the use of nanomaterials to modify the electrode surface, including the ones obtained from renewable sources, such as CNM.[180−182] The great interest in applying CNM in electrical and electrochemical sensors is due to its advantageous features, which include thermal stability,[183,184] high aspect ratio,[37] good mechanical and optical properties, and large surface area.[185] Besides, cellulose is an excellent bonding agent, as it has readily available surface functional groups, which can provide selectivity and sensitivity compared to other molecules with no functional groups available, with impact on the long-time stability of the modified electrode.[186−188] Table 2 summarizes some interesting electrochemical and electrical (bio)sensors based on CNM and its characteristics.

Silva et al.[80] reported the application of BC nanosheets as a proof-of-concept skin-like platform for noninvasive monitoring of body fluids in sweat using screen-printed carbon electrodes (SPCEs). BC is an excellent skin-substitute natural polymer routinely used for wound dressing and offers unprecedented potential as a substrate for wearable sensors. The sensing platform obtained with BC can help in solving the adhesion problem, thus allowing skin integration in wearable devices. The electrodes were used to detect the toxic metals cadmium (Cd^{2+}) and lead (Pb^{2+}) with limits of detection of 1.01 and 0.43 μM, respectively, which are sufficient to detect these metal ions in human sweat and urine. SPCEs functionalized through anodic pretreatments were used for detecting uric acid and 17β-estradiol in artificial sweat, with detection limits of 1.8 μM and 0.58 μM, respectively. The electrochemical treatment created oxygen groups on the carbon surfaces, thus improving wettability and hydrophilicity. The authors achieved a detection limit similar to other works reported in the literature[199−202] but using BC as a highly adherent biocompatible skin-like platform, which can transport species such as toxic metals from sweat to the printed carbon ink through a capillary effect.

Another interesting approach was proposed by Zheng et al.,[203] who developed a new class of strain sensors using CNF and graphene (GN) coincorporated poly(vinyl alcohol)-borax (GN-CNF@PVA) hydrogel. The borax could reversibly and dynamically associate with poly(vinyl alcohol) (PVA) and GN-CNF nanocomplexes, acting as a cross-linking agent, providing a tough and flexible network with the hydrogels. In this case, the CNF acted as a biotemplate and dispersant to support GN to create homogeneous GN-CNF aqueous dispersion, endowing the GN-CNF@PVA gels with mechanical flexibility, strength, and conductivity. The resulting composite gels presented remarkable stretchability (breakup elongation up to 1000%), excellent viscoelasticity (storage modulus up to 3.7 kPa), rapid self-healing ability (20 s), and high healing efficiency (97.7 ± 1.2%). Due to the effective electric pathways provided by GN-CNF nanocomplexes, the strain sensors integrated by GN-CNF@PVA hydrogel with good responsiveness, stability, and repeatability could identify various human motions with the gauge factor (GF), showing promising applications in the field of wearable sensing devices. These results are presented in Figure 3A, where it is possible to observe transmission electron microscope (TEM) images of CNF (i), GN (ii), and GN-CNF nanocomplexes (iii), and (iv) macroscopic pictures of pure GN and GN-CNF dispersions after a 12 h rest.

A novel electrochemical sensor for detecting Hg^{2+} using a green hybrid nanoarchitecture composed of reduced graphene oxide (rGO), CNC, and polyamide 6 (PA6) electrospun nanofibers was developed by Teodoro et al.[45] In this work, the CNC were used as an alternative reducing agent for graphene oxide (GO). The surface molecules of cellulose led to a partial reduction of oxygen organic functions of graphene oxide, resulting in well-dispersed rGO onto the CNC surface. The CNC:rGO hybrid material was applied in the functionalization of insulating electrospun nanofibers deposited onto the working electrode. The results revealed that the sensor was capable of detecting Hg^{2+} with a low limit of detection (LOD) of 0.52 μM in a concentration range of 2.5−200 μM. Figure 3B(i) shows the DPV curves for different concentrations of Hg^{2+} using the PA6/CNC:rGO hybrid platform, in 0.1 mol L^{-1} acetate buffer, and (ii) shows the linear relationship between the peak current versus Hg^{2+} concentrations. The proposed sensor also proved to be selective in the presence of common interfering metals (Cd^{2+}, Pb^{2+}, and Cu^{2+}) and was able to detect Hg^{2+} in real samples, including in river and tap water. Regarding electrical sensors using cellulose material, Migliorini et al.,[189,204] in two different studies, evaluated the performance of nanocomposites based on electrospun nanofibers modified by CNC hybrid materials with AgNP, AuNP, and rGO to be used as sensing layers of an electronic tongue (e-tongue) to detect water contaminants. In these two works, the use of CNC in the synthesis of CNW:Ag and CNC:Au hybrid materials allowed obtaining small and well-dispersed metal nanoparticles onto the electrospun nanofibers surface, which would not be achievable without using CNC. In another approach, Ivanova et al.[112] developed a resistive gas sensor based on CNC templated tin dioxide. The authors demonstrated that the structural features of CNC-templated tin dioxide films strongly depend on the precursor composition. The precursor properties were studied by using low-temperature NMR spectroscopy of tin tetrachloride in solution. In addition, they also demonstrated that it was possible to optimize the precursor conditions to obtain homogeneous precursor mixtures and therefore highly porous thin films with pore dimensions in the range of 10−20 nm. The sensor showed high sensitivity to carbon monoxide (CO) in ppm concentrations and low cross-sensitivity to humidity. Besides, both the response to the analyzed gas and the signal decay after gas exposure occurred within a few seconds, which is faster than in standard SnO_2-based CO sensors, which was attributed to the high gas accessibility of the very thin porous film.

In the work reported by Migliorini et al.,[189] nanocomposites based on electrospun nanofibers modified with the hybrid materials CNC:AgNP, CNC:AuNP, and CNC:rGO were employed in the design of an e-tongue sensor array, in order

https://doi.org/10.1021/acssensors.1c00473
ACS Sens. 2021, 6, 2473−2496

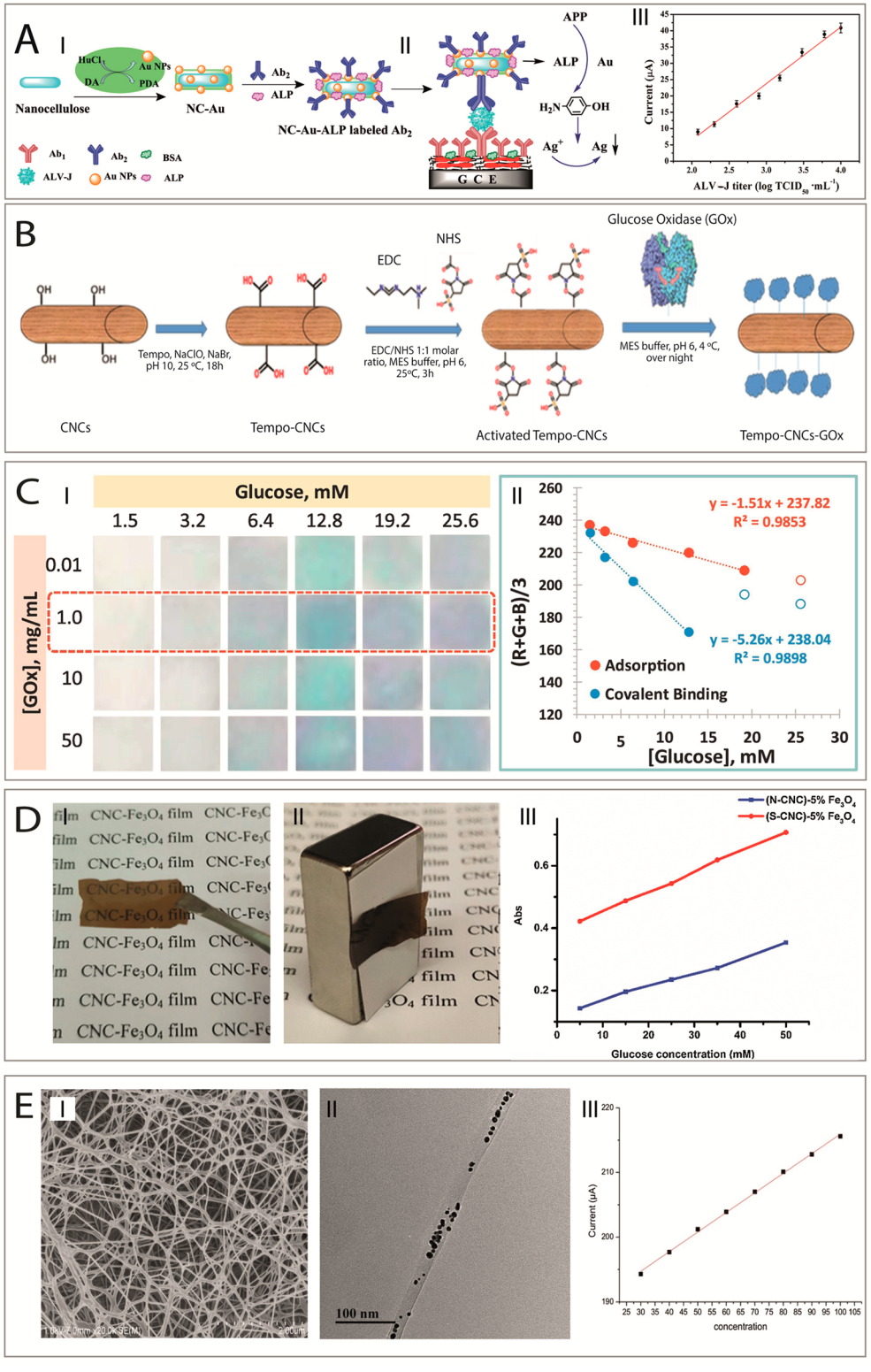

Figure 4. (A) Design strategy used in the fabrication of CNM-AU-Ab_2-ALP (I), the sandwich-type immunosensor (II) and the calibration curve for ALV-J detection (III). Adapted with permission from ref 218. Copyright 2018 Elsevier. (B) Schematic view of the TEMPO−CNC oxidation and enzyme immobilization process. Adapted with permission from ref 195. Copyright 2018 Elsevier. (C) Digital images of the test-strips in the presence of different glucose concentrations using ABTS as colorimetric indicator, prepared with different concentrations of GOx covalently bound (I) and the analytical calibration curves (II) plotting the color coordinates collected against the glucose concentration (right − the assay corresponds to 1 mg mL^{-1} GOx). Adapted with permission from ref 58. Copyright 2020 Elsevier. (D) Translucency (I) and magnetic property (II) of the self-supporting S-CNC-5% Fe_3O_4 film, and the dependence of (N-CNC)-5% Fe_3O_4 and (S-CNC)-5% Fe_3O_4 catalytic activity on glucose concentration (III). Adapted with permission from ref 224. Copyright 2020 Elsevier. (E) SEM image of BC nanofibers (I), TEM image of BC-AuNP hybrid nanofiber (II), and calibration curve of current vs concentration for hydroquinone detection (III). Adapted with permission from ref 197. Copyright 2016 Elsevier.

https://doi.org/10.1021/acssensors.1c00473
ACS Sens. 2021, 6, 2473−2496

to detect isoborneol, a compound associated with the eutrophication process. Additionally, electrical capacitance data measured with the impedimetric e-tongue were treated by Principal Component Analysis (PCA) and revealed that the sensing system was able to discriminate water samples contaminated with isoborneol at nanomolar concentrations (Figure 3C), even when real water samples were employed. In a sequential work, the same authors[204] evaluated two distinct e-tongues to detect geosmin (GSM) and 2-methylisoborneol (MIB) in pure and river water. The difference between the e-tongues consisted in the type of polymer processing (electrospinning or drop-casting) used in the fabrication of the sensing units. Specifically, the thin films deposited onto gold interdigitated electrodes were based on polyamide 6, polypyrrole, and polyaniline, but fabricated by drop-casting and electrospinning. The drop-casting and electrospinning were further functionalized with well-dispersed CNC:Ag and CNC:Au hybrids. The differences in the electronic tongue performances were correlated to the distinct morphologies of the sensitive layers. Both devices were able to discriminate pure water from solutions tainted with GSM and MIB in concentration as low as 25 ng L^{-1}. In addition, the system showed intra- and interelectrode reproducibility and the performance similar to that reported by Braga et al.,[205] but in that case[204] using a green synthesis based on CNC.

In another approach, Annu et al.[190] developed a cellulose-modified pencil graphite electrode to quantify the herbicide atrazine (ATZ). As pointed out by the authors, CNM find several applications in electrochemistry owing to the large number of hydroxyl groups on its structure, combined to chemical purity and, in the specific case of this work, easy distribution/dispersion and good adsorption on electrode surface and reinforcing phase capabilities. The fabricated sensor could detect ATZ with a low detection limit of 0.008 ng mL^{-1} without interference of common metabolites. By comparing the results achieved by his team[190] with other studies reported in the literature,[206−208] one notes the proposed sensor presented equal or superior sensitivity with the advantage of being a cost-effective sensor and easy to fabricate, demonstrating that it could be a potential green substitute for conventional pencil graphite electrodes.

Cellulose Nanomaterials in Biosensors. A biosensor is a type of chemical sensor that uses a biological molecule as a recognition element. When nanomaterials are employed in biosensors, interesting catalytic properties for detecting varied analytes are observed.[209] Besides, nanomaterials can be tailored allowing improvements in the immobilization and stabilization step of biological components (enzyme, antibody, aptamers, nucleic acids, etc.), which are key elements for efficient recognition of the target analyte.

Biosensors using nanostructured hybrid materials can be employed for different applications such as environmental monitoring,[210,211] food industry,[212,213] and health care.[214,215] The latter application, which includes wearable sensors for disease diagnosis and in vivo health monitoring, raises concerns about the possible cytotoxicity of nanomaterials. To overcome this problem, biocompatible nanomaterials, as CNM, are a suitable option to be applied in biosensors for in vivo detection of varied analytes.[8,216] CNC, CNF, and BC have been widely applied in biosensing development[8] due to their remarkable properties mentioned in the previous sections combined with nontoxicity and biocompatibility, which are key for wearable biosensors. Although CNM's biodegradability is advantageous for some cases regarding in vivo applications, some concerns are raised when CNM is acting as a support material for other nonbiodegradable materials, which can be delivered after its CNM degradation.

Regarding biosensors development, CNM have been applied as reinforcement agents of biocomposites,[194,196,217,218] as biocompatible interface former,[80,219,220] as a substrate for biomolecule immobilization[58,195,221−223] and in the design of self-supporting devices.[22,95,224] Regarding applications, considering that CNM are natural and nontoxic nanomaterials, they can be applied in sensors aimed at food quality control[95,210] and health monitoring,[106,225] especially in the development of point-of-care and wearable devices.[80,196,219,224,226] At first, CNM-based devices were intended to replace the glass or plastic-based devices, but their use offers interesting additional advantages, as in the development of (nano)paper-based support for (bio)sensors, leading to cost-effective, reliable, sustainable, and reagent-free devices applied in food quality and safety monitoring.[95] In addition, its low cost allows the production of disposable devices, overcoming fouling issues found in food quality application. Regarding the environmental impact, the use of CNM-based devices brings sustainability and also allows recycling. The development of devices based on CNM also represents a great advantage in the microfluidic field, where the paper porosity and capillarity effects can be used for the production of miniaturized devices that require small analyte volumes without the need of micropumps, avoiding bubble formation.[95,106] Besides, the biocompatibility and nontoxicity of CNM-based biosensors and the possibility of functionalization allows the successful immobilization of several biological compounds.[106,225]

CNM can be associated with inorganic nanoparticles,[194,227] metal ions and oxides,[192,218] carbon-based materials (nanotubes, graphene, graphene oxide, etc.),[228−230] conducting polymers,[231,232] and ionic liquids,[233] to improve conductive and electrochemical properties[217] of the nanocomposite. For example, Liu et al.[218] developed an electrochemical immunosensor using a composite formed by CNM and AuNP, named CNM/AuNP, for the detection of avian leukosis virus subgroup J (ALV J). The designed immunosensor was produced following a sandwich-type scheme, where ALV J, the target molecule, was recognized between two nanocomposites with immobilized primary and secondary antibodies, namely, Ab1 and Ab2, respectively (a secondary antibody is an antibody that recognizes a primary antibody). Figure 4A(I) and (II) show a scheme of the designed immunosensor, where Ab1 is the capture antibody and Ab2 is the detection antibody. The first nanocomposite was formed by a Graphene/perylene-3,4,9,10-tetracarboxylic acid (GR/PTCA) and the second one by CNM/AuNP. CNM were used as matrix for AuNPs immobilization in order to enhance the electrochemical immunosensors performance, in addition to functioning as a carrier to immobilize the antibody Ab2 and alkaline phosphatase molecules (ALP), which acts as a catalyst. The formation of CNM-Au composites allowed the amplification of the detected signal and favored the catalytic properties of Au and ALP. The calibration curve for the developed immunosensor is shown in Figure 4A(III). The sensor showed a LOD (calculated by S/N = 3) of $10^{1.98}$ $TCID_{50}$ mL^{-1} ($TCID_{50}$ = 50% tissue culture infective dose), adequate selectivity (according to interference tests using relevant species as vitamin C, glucose, BSA, NaCl, etc.) and reproducibility (RSD = 2.01%). Besides, the developed sensor showed long-term

https://doi.org/10.1021/acssensors.1c00473
ACS Sens. 2021, 6, 2473−2496

stability, keeping 93.57% of the peak current detection signal after 15-day storage.

Manan et al.[194] reported the fabrication of an electrochemical biosensor using CNC decorated with cadmium sulfide quantum dots (CdS QDs) for immobilizing Tyrosinase (Tyr), aiming at phenol detection. The surface modification of CNC was performed using the cationic surfactant cetyltriammonium bromide (CTAB) in order to overcome its high hydrophilicity and render a moderate hydrophobicity to the biosensor matrix. After functionalization, the modified CNC were successfully used for CdS QDs (capped with 3-mercaptopropionic acid − MPA-QDs) attachment and Tyr immobilization. The CdS QDs provided conductivity and facilitated the electron transfer to the system, while Tyr catalyzed phenol reduction to *o*-quinone. The Tyr/CTAB-CNM/QDs biosensor exhibited a good linear response (R^2 = 0.9904) in the concentration range of 5−40 μM showing an LOD of 0.082 μM toward phenol detection. Besides, the developed biosensor showed selectivity for phenol determination in the presence of common interferents (10 times concentration of glucose, ascorbic acid, uric acid, caffeine, and 100 times concentration of heavy metal ions), presenting less than 5% of interference and accuracy comparable with results obtained by HPLC. An efficient immobilization capable of ensuring the exposition of the active sites for the necessary binding is one of the main challenges in biosensing applications.[234] In the case of CNM, the surface modification is an efficient strategy used for designing the adequate binding of biological molecules on its surface for biosensors development. For instance, the use of the oxidant agent 2,2,6,6-tetramethylpiperine-1-oxyl (TEMPO) as a mediator in the oxidation process is a widely used and promising procedure.[58,192,195] It enables oxidation of primary hydroxyl groups from cellulose in aldehydes, which are further converted (using other reagents) into charged carboxyl groups.[235,236] The process is advantageous for being one-step and specific for primary alcohol groups of polysaccharides, keeping secondary ones unaffected.[237] In this direction, a biocompatible and inert nanomaterial based on TEMPO oxidized-CNC, used for immobilizing and stabilize glucose oxidase (GOx), was designed by Tang et al.[195] The TEMPO-mediated oxidation process enabled the hydroxyl groups of CNC to be oxidized into carboxyl groups, for which the surface chemical functionalization allowed the covalent bonding of the GOx through the reaction with the NHS/EDC (*N*-hydroxysuccinimide/*N*-(3-(dimethylamino)propyl)-*N*′-ethylcarbodiimide) reagents, leading to an effective enzyme immobilization. Figure 4B shows a schematic view for the derivative procedure and GOx immobilization. The sensor was fabricated on a screen-printed electrode and exhibited a linear range of detection from 0.1 to 2 mM (R^2 = 0.999), LOD of 0.004 mM, and limit of quantification of (LOQ) 0.012 mM. The as-prepared platform was successfully used for monitoring the glucose concentration (consumption) of a fibroblast cell culture medium.

In another strategy, Neubauerova et al.[58] developed a glucose colorimetric biosensor using CNM deposited onto a cellulose paper substrate. Specifically, the authors used MCC as a cellulose source, which was oxidized using TEMPO-mediated oxidation, leading to the formation of carboxylated groups at the cellulose surface. Next, CNC were extracted by acid hydrolysis and then cast onto a cellulose substrate to support glucose oxidase (GOx), horseradish peroxidase (HRP), and 2,2′-azino-bis(3-ethylbenzothiazoline-6-sulfonic acid) diammonium salt (ABTS). The colorimetric sensing mechanism was based on the HRP and ABTS action on hydrogen peroxide (H_2O_2), produced from the reaction between GOx and glucose, generating a blue product. Figure 4C(I) shows the digital images of the developed biosensor test-strips in the presence of different concentrations of glucose and GOx, while Figure 4C(II) shows the analytical calibration curves plotting the color coordinates against the glucose concentration (1 mg mL^{-1} of GOx). The authors observed that modified CNM promoted better color distribution and increased sensitivity (3.5 times higher) for glucose detection, in which a narrower linear response range from 1.5 to 13.0 mM was obtained.

Recently, noninvasive wearable biosensors have gained considerable interest owing to their plethora of applications.[177,238−240] Improvements in the performance of wearable devices have been achieved by using both cellulose-based membranes (to avoid the interference from other biofluid compounds in on-body applications of glucose detection[219]), as well as CNM. In this direction, Burrs and collaborators developed a conductive nanopaper based on a graphene−platinum (Pt) nanocauliflower hybrid composite for use in point-of-care biosensing for glucose or *Escherichia coli* (*E. coli*) detection.[196] First, the device was fabricated through nanocellulose modification with graphene oxide, which was reduced by subsequent thermal and chemical (using ascorbic acid) treatment, constituting an interesting conductive substrate for electrochemical measurements. After that, the surface of the substrate was modified through the synthesis and application of fractal nanoplatinum with cauliflower-like morphology using pulsed sonoelectrodeposition, and a high electroactive surface area was achieved. The platinum surface was further modified with the enzyme GOx (via chitosan encapsulation) or an RNA aptamer (via covalent linking) for the development of an enzymatic biosensor or aptasensor in the detection of glucose or *E. coli*, respectively. The results showed that the hybrid nanocellulose−graphene−nanoplatinum material is an excellent paper-based platform for electrochemical biosensors targeting small molecules.

A different strategy was employed by Tracey et al.,[224] who reported the development of a noninvasive glucose biosensor based on CNC/magnetite for in vivo or dermal use. In that work, the properties of CNC to form self-supporting and biocompatible films were employed for the biosensing of glucose from sweat and saliva. For the film formation, nonsulfated cellulose nanocrystals (N-CNC) were isolated, and sulfated cellulose nanocrystals (S-CNC) were produced by partial esterification of CNC surface hydroxyl groups using sulfuric acid. Both materials were associated with magnetite (Fe_3O_4) in the development of hybrid composites for the formation of (N-CNC)-Fe_3O_4 and (S-CNC)-Fe_3O_4 hybrid system casting films. A colorimetric transduction system was explored by immobilizing GOx and ABTS in the hybrid films strips. Briefly, the H_2O_2 molecules from GOx/glucose reacted with ABTS that was oxidized through the catalyst action (peroxidase-like) of magnetite, and as a result, the color of the film changed. Figure 4D shows the developed self-supporting biosensor and (I) its translucency and (II) its magnetic properties. Both proposed that hybrid biosensors displayed peroxidase-like activity (reducing H_2O_2 and oxidizing ABTS) and were capable of detecting glucose concentrations as low as the level of glucose in biological fluids (5 mM). Figure 4D(III)

https://doi.org/10.1021/acssensors.1c00473
ACS Sens. 2021, 6, 2473−2496

shows the calibration curve on glucose detection for the developed biosensors. The color change was almost immediate, and the (S-CNC)-Fe_3O_4 platform was 1.5−2 times more reactive than (N-CNC)-Fe_3O_4.

BC nanofibers have also been used in the development of biosensors due to their three-dimensional (3D) nanostructure and high degree of crystallinity, which favors the adsorption of nanomaterials and biological compounds. In this sense, Li et al. used BC nanofibers in the development of a biosensor for hydroquinone detection.[197] Figure 4E(I) shows the BC 3D structure which was produced by *Gluconacetobacter xylinum* bacteria. After that, a nanocomposite was formed using BC-Au nanoparticles (NP) by electrostatic assembly and in situ chemical reduction methods. The BC-AuNP structure formed is displayed in the TEM microscopy image of Figure 4E(II), which shows that the BC nanofibers were successfully coated with AuNP. A glassy carbon electrode (GCE) was modified with BC-AuNPs, and the enzyme laccase (Lac) was then immobilized on its surface with Nafion, forming the GCE-Nafion-BC-AuNPs-Lac biosensor. Hydroquinone was detected using the DPV method, and a low LOD of 5.71 nM and a linear analytical range was found for concentration of 30−100 nM, as shown in Figure 4E(III). Moreover, the device was employed for hydroquinone determination in real samples (tap and lake water) showing that is a promising sensing platform for environmental pollutant.

Cellulose Nanomaterials in Piezoelectric Sensors. Piezoelectricity has been a property of interest for the design of pressure and strain sensors, which have recently attracted great attention for applications in human health monitoring, smart devices, human−machine interaction, and wearable electronics.[241] As previously mentioned, the piezoelectricity of cellulose and wood has been known for decades, and more recently has also been demonstrated in CNC films, with comparable performance to the reference metal oxide film.[124] In this scenario, CNM has been highly explored in advanced devices as nanogenerators, actuators, gas and humidity sensors, biosensors, and piezoelectric fillers for strain sensors. Such devices find applications in environmental and human physiological signal monitoring, such as speech recognition and real-time wrist pulse monitoring.[242−244] Table 3 summarizes some examples of CNM-based piezoelectric sensors used for detecting motion.

The enhancement of piezoelectricity in isolated crystalline parts of cellulose, i.e., CNC,[245] combined with biocompatibility, has led to the large use of CNM in piezoelectric systems.[22,125] For instance, Yun et al.[246] demonstrated that the application of an electric field in aligned cellulose films could induce the formation of nanofibers and, by consequence, increase their crystallinity. This effect played the main role in the enhancement of piezoelectricity, reaching a value of 10.6 ± 0.77 pC N^{-1}, higher than the in-plane piezoelectric charge constant of ordinary poly(vinylidene fluoride) (PVDF) films. Csoka et al.[124] experimentally showed the piezoelectricity of CNC in thin films, which could be further increased with the degree of alignment of the CNC in the films. The higher piezoelectric constant value of 2.10 Å/V obtained for the CNC film with a degree of alignment of 88% was superior to that of the reference film of ZnO (1.3 Å/V). In another strategy, electrospinning PVDF with CNC resulted in a nanocomposite with superior piezoelectric properties compared to those of pure PVDF nanofibers.[247,248] In addition, the combination of CNM with ZnO,[249] polydimethylsiloxane (PDMS),[250] and chitosan[251] to obtain piezoelectric devices has been reported.

Table 3. Examples of Cellulose-Based Piezoelectric Sensors Used for Detecting Motion

type of sensor	materials	sensitivity[a]	ref
Force	Natural cellulose nanofibrils	4.7−6.4 pCN^{-1}	245
Pressure	TEMPO-oxidized cellulose nanofibril	500 Pa−3 kPa	256
Strain	Carbon nanotube, cellulose nanocrystals, and polyurethane membrane	GF = 321	257
Strain	Cellulose nanofibrils, silver nanowire, and polyurethane sponge	GF = 26.07	254
Pressure	$BaTiO_3$, multiwalled carbon nanotubes, and bacterial cellulose	2 kPa	258
Strain	Waterborne polyurethane, carbon nanotube, and cellulose nanocrystal	GF = 1	259
Pressure and proximity	Porous silver nanowire-bacterial cellulose fiber	5.49 MPa^{-1}	260
Strain	Silver nanoparticles, carbon nanotubes, cellulose nanocrystals, tannic acid, and polyurethane	GF = 17.1	255

[a]GF = Gauge factor.

In piezoelectric sensors,[22,245,246,252] mechanical changes are converted into electrical signals to be further analyzed. Most of the works using CNM in piezoelectric sensors are dedicated to detecting motion, i.e., pressure, flow, vibration, strain, etc.[119,253] Some recent examples of works using CNM in piezoelectric motion sensors are also shown in Table 3. For example, Zhang et al.[254] used cracked CNF and silver nanowire (AgNW) to coat a polyurethane (PU) sponge and endowed it with piezoresistive properties. The use of CNF was important to enable the dispersion of the AgNWs and facilitate the adhesion of the conductive layer and the PU skeleton. The electrical conductivity and mechanical properties of the material were investigated and could be tuned based on the amount of CNF and AgNWs coated onto the sponge. The piezoresistive sensor functioning was based on the application of pressure or strain, leading to a rearrangement of the conductive network and consequent changes in the electrical resistance. The sensor was able to detect human body motion with different strains. Furthermore, the potential of using the material as an artificial electronic skin was demonstrated by showing the ability of the sensor to detect the shape and location of an object, as shown in Figure 5A. In another work, Yan et al.[255] also used a PU sponge decorated with CNC, AgNP, carbon nanotubes (CNT), and tannic acid (TA) to obtain an ultrasensitive and highly compressive piezoresistive sensor. The brittle CNC were employed to disperse the CNT and formed a microcracked structure providing a sensor with high sensitivity toward small compressive strains. The piezoresistive sensor presented good stability and stable mechanical compressive recoverability for gentle and large deformation tests, as shown in Figure 5B(I). For consecutive 150 cyclic compressive tests at a strain of 1%, 40%, and 80% applied to the material, the relative resistance increased according to the strain applied and went back to 0% with the stress release. Such comportment shows that the AgNPs/CNTs−CNCs@TA−PU sponge can be used for fabricating piezoresistive sensors. The material was applied in the monitoring of different human motions. As shown in Figure

https://doi.org/10.1021/acssensors.1c00473
ACS Sens. 2021, 6, 2473−2496

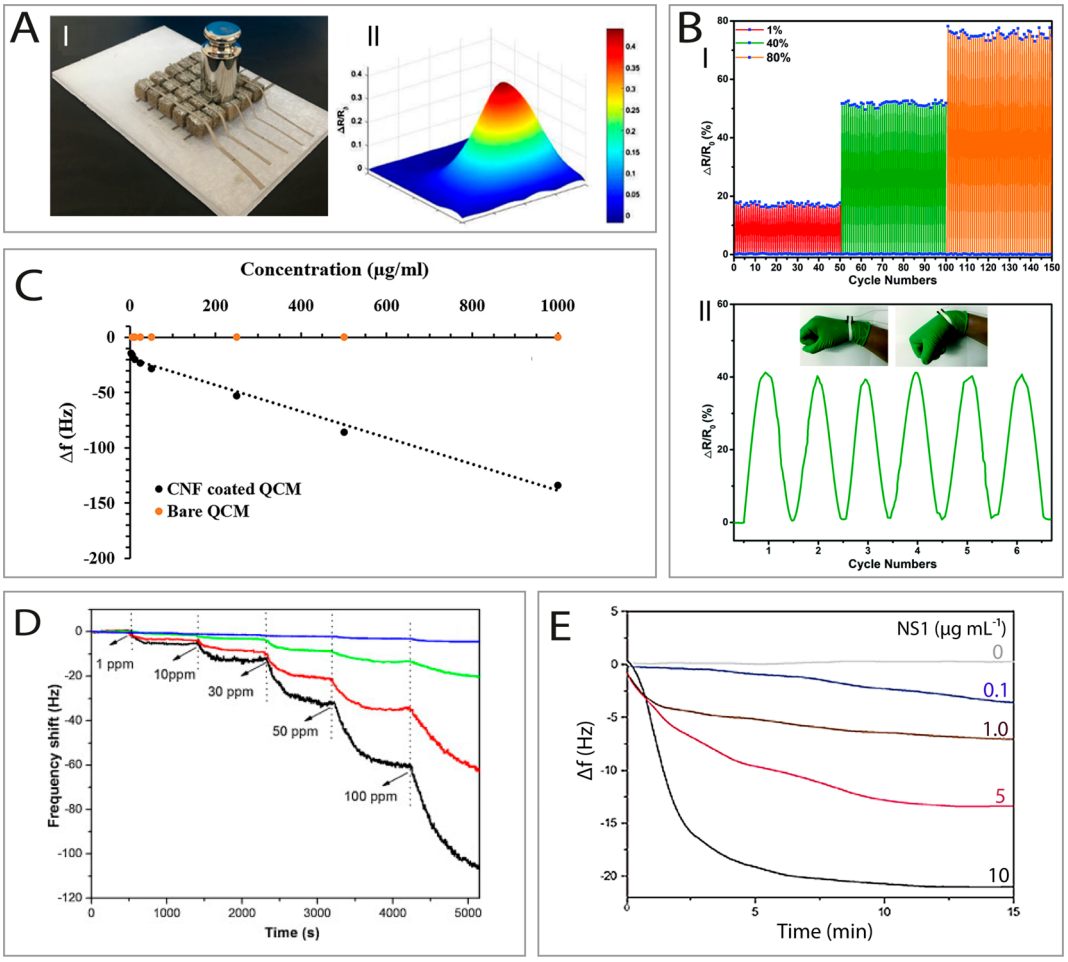

Figure 5. (A) (I) Digital photograph of the PU sponge coated with CNF and AgNW used as an artificial electronic skin, with a 100 g weight on it and (II) the corresponding map of estimated pressure profile based on the change in resistance. Adapted and reproduced with permission from ref 254. Copyright 2019 The American Chemical Society. (B) (I) Stability test of the piezoresistive behavior of AgNPs/CNTs−CNC@TA−PU sponge under a compression strain of 1%, 40%, and 80% and (II) detection of wrist bending by the piezoresistive sensor. Adapted and reproduced with permission from ref 255. Copyright 2020 Royal Society of Chemistry. (C) Frequency shifts versus glycine concentration in the presence of the CNF-coated QCM and unmodified QCM. Adapted and reproduced with permission from ref 267. Copyright 2020 Springer Nature. (D) Response of the quartz crystal microbalance coated with BC membrane (blue), PEI membrane (green), and PEI/BC membranes with a weight ratio of 0.67/1 (red) and 1.34/1 (black). Adapted and reproduced with permission from ref 268. Copyright 2011 Elsevier. (E) Detection of the antigen NS1 in diluted blood serum by the immunoglobulin G immobilized on the surface of QCM coated with cellulose through the frequency shift related to the amount of NS1 in the solution. Adapted and reproduced with permission from ref 223. Copyright 2017 Elsevier.

5B(II), the sensor was adhered to the wrist and could detect repeated bending action with excellent stability and repeatability, revealing its potential for use as a wearable piezoresistive sensor.

CNM have also been used in the composition of a quartz crystal microbalance (QCM),[261] a mass sensor based on the piezoelectric effect of quartz, in which changes in its resonance frequency are used to determine the amount of mass present on the crystal.[262−264] The sensitivity of a QCM can be enhanced by coating the quartz with appropriate materials to provide specific interactions with varied analytes or using sensing materials with a high specific surface area.[262,263,265] For instance, Yao et al.[266] developed a humidity QCM sensor based on the asymmetric electrode structure and CNC as the sensing material. The detection of humidity by the sensor occurred through the changes in mass and in the dielectric constant of the CNC films due to the adsorption of water by the CNC. The high adsorption capability was attributed to the abundant hydrophilic functional groups presented by the CNC. The CNC based QCM humidity sensor presented high stability in the low and middle humidity range (<84.3%). The detection of glycine was performed by Hosseini et al.[267] using CNF to coat the quartz crystal of the sensor. A thin layer of the sensing material was prepared by spin-coating a CNF suspension onto the electrode, resulting in a full-coverage film with stability and wettability. As an advantage, the CNF did not require any further modification to adsorb the glycine molecules. The sensing mechanism was attributed to the formation of hydrogen bonds between the CNF and the analyte. As shown in Figure 5C, the QCM without the CNF produced no frequency change in the presence of glycine, while the CNF-based QCM showed a linear frequency decrease with the increase of glycine concentration, from 6 to 500 μg mL^{-1}, presenting a LOD of 8 μg mL^{-1}.

Hu et al.[268] used BC to enhance the sensitivity of a QCM to detect formaldehyde, based on its large surface area and high porosity. Polyethylenimine (PEI) was used with BC to produce a nanofibrous membrane employed as the sensing

https://doi.org/10.1021/acssensors.1c00473
ACS Sens. 2021, 6, 2473−2496

material. Figure 5D shows the synergic effect of BC and PEI in the detection formaldehyde when the sensor was exposed to various concentrations of formaldehyde. Compared with previously reported works[269,270] that also used PEI in the composition of the sensing material, the authors showed that incorporation of BC led to higher sensitivity and a lower LOD of 1 ppm, and faster response. The superior performance was attributed to the high specific surface area of the membrane. Furthermore, the sensor was tested against conventional VOCs, such as dichloromethane, tetrahydrofuran, trimethylamine, toluene, ethanol, benzene, and trichloromethane at 100 ppm, and showed very small sensitivity toward ethanol and no sensitivity toward the other gases, revealing its good selectivity. In addition, the sensor was subjected to a test of reproducibility and reversibility by completely desorbing the formaldehyde and then treating again with the previously used concentration. The result presented nearly the same frequency shifts before and after the desorption of formaldehyde, confirming the high reversibility and good reproducibility for the sensor toward formaldehyde molecules.

Pirich et al.[223] used a QCM coated with thin films of bacterial CNC to immobilize monoclonal immunoglobulin G (IgGNS1) and perform a specific detection of the dengue fever protein 1 (NS1). The carboxyl groups of the CNC provided an easy and reliable alternative to immobilize bioactive molecules and a porous surface that increased the available area to immobilize the IgGNS1, which increased the sensitivity of the piezoelectric sensors. The authors performed the recognition of the NS1 in PBS and blood serum (ten times diluted in PBS), reaching a LOD of 0.002 and 0.10 μg mL^{-1}, respectively, for a QCM with dissipation monitoring. Figure 5E shows the frequency shift of the QCM with dissipation monitoring for the NS1 recognition by the IgGNS1 immobilized on the cellulosic surface in diluted blood serum, showing its potential to be used in clinical dengue diagnosis during the intense phase of the disease.

CONCLUSIONS AND FINAL REMARKS

Herein, we reviewed the fascinating properties of CNM, including cellulose nanocrystals (CNC), cellulose nanofibrils (CNF), and bacterial cellulose (BC), that give them potential for the design of sensors and biosensors for detecting varied analytes. Specifically, the CNM materials show many interesting properties such as molecular polarization, electrostatic interactions, and switchable hydrogen bonds. Other remarkable properties include high specific surface area, renewability, nontoxicity, biocompatibility, and low cost. More recently, the association of CNM with other nanomaterials (e.g., metallic nanoparticles, carbon-based nanomaterials, enzymes, etc.) has driven the development of a large number of cellulose-based nanocomposites and hybrid materials in the form of papers, gels, thin films, membranes, and liquid suspensions. Such a strategy appears to be an affordable trend for designing multifaceted optical, electrical, electrochemical, and piezoelectric sensors and biosensors for detecting physiological parameters and environmental pollutants.

Even though CNM-based optical sensors have experienced a rapid advance, they usually do not present the same performance in terms of the limit of detection and sensitivity compared to their electrical and electrochemical counterparts. Besides, CNM-based optical sensors are usually more susceptible to suffering interference from common interferents, considering that in many cases the detection mechanism is based on color changes arising from a swelling process that enlarges the helical pitch of the cellulose chiral nematic structure. Therefore, for all the cases, in order to achieve higher selectivity for cellulose-based sensors, a judicious choice of the nanomaterials should be taken.

In the last years, emphasis has been given to the development of CNM-based wearable sensors for in vivo analysis of human diseases and physiological parameters, taking advantage of CNM nontoxicity, biocompatibility, and chemically versatile properties. Therefore, it is expected that such CNM-based wearable sensors can in part overcome some shortages of traditional analytical systems, which usually demand bench equipment as well as extraction of fluids for in situ analysis of physiological parameters. One important aspect that can limit the use of CNM in sensors (as well as in other devices) is related to the cost of production and purity of the as-obtained material. In the case of BC, larger-scale production is still challenging, and the quality of the end product depends on the specific bacteria strains as well as feedstocks employed. For CNF, the costs are more related to the type of pretreatment employed, where the more affordable one is the enzymatic pretreatment process. Therefore, we believe this process might be useful for large-scale production of disposable CNM-based sensors made of pristine CNM or even CNM-based composites. For CNC, the most employed method is based on the use of a sulfuric acid hydrolysis method, which is commercially available and has enabled the use in some medical products, with potential for wearable sensors. In summary, although some important bottlenecks still need to be overcome, recent and continuous advances in the scalability of industrial production of some types of CNM and CNM-based composites point out for their utilization in the design of optical, electrical, electrochemical, and piezoelectric sensors in the middle and long-term.

AUTHOR INFORMATION

Corresponding Author

Daniel S. Correa − *Nanotechnology National Laboratory for Agriculture, Embrapa Instrumentação, 13560-970 São Carlos, São Paulo, Brazil; PPGQ, Department of Chemistry, Center for Exact Sciences and Technology, Federal University of São Carlos (UFSCar), 13565-905 São Carlos, São Paulo, Brazil;* orcid.org/0000-0002-5592-0627; Email: daniel.correa@embrapa.br

Authors

Kelcilene B. R. Teodoro − *Nanotechnology National Laboratory for Agriculture, Embrapa Instrumentação, 13560-970 São Carlos, São Paulo, Brazil;* orcid.org/0000-0003-4337-4849

Rafaela C. Sanfelice − *Science and Technology Institute, Federal University of Alfenas, CEP 37715-400 Poços de Caldas, Minas Gerais, Brazil;* orcid.org/0000-0002-2176-7177

Fernanda L. Migliorini − *Nanotechnology National Laboratory for Agriculture, Embrapa Instrumentação, 13560-970 São Carlos, São Paulo, Brazil;* orcid.org/0000-0002-9605-2790

Adriana Pavinatto − *Scientific and Technological Institute of Brazil University, São Paulo 08230-030, Brazil;* orcid.org/0000-0003-1370-9070

https://doi.org/10.1021/acssensors.1c00473
ACS Sens. 2021, 6, 2473−2496

Murilo H. M. Facure − *Nanotechnology National Laboratory for Agriculture, Embrapa Instrumentação, 13560-970 São Carlos, São Paulo, Brazil; PPGQ, Department of Chemistry, Center for Exact Sciences and Technology, Federal University of São Carlos (UFSCar), 13565-905 São Carlos, São Paulo, Brazil;* orcid.org/0000-0003-0858-0364

Complete contact information is available at: https://pubs.acs.org/10.1021/acssensors.1c00473

Notes

The authors declare no competing financial interest.

■ ACKNOWLEDGMENTS

The authors thank the financial support from Fundação de Amparo à Pesquisa do Estado de São Paulo (FAPESP) (grant numbers: 2017/12174-4, 2017/10582-8, 2017/21791-7, 2018/22214-6, 2017/19470-8), Conselho Nacional de Desenvolvimento Científico e Tecnológico (CNPq), MCTI-SisNano (CNPq/402.287/2013-4), Coordenação de Aperfeiçoamento de Pessoal de Nível Superior - Brasil (CAPES) - Código de Financiamento 001 and Rede Agronano-EMBRAPA from Brazil.

■ REFERENCES

(1) Teymourian, H.; Parrilla, M.; Sempionatto, J. R.; Montiel, N. F.; Barfidokht, A.; Van Echelpoel, R.; De Wael, K.; Wang, J. Wearable Electrochemical Sensors for the Monitoring and Screening of Drugs. *ACS Sensors* **2020**, *5* (9), 2679−2700.

(2) van der Zalm, J.; Chen, S.; Huang, W.; Chen, A. Review—Recent Advances in the Development of Nanoporous Au for Sensing Applications. *J. Electrochem. Soc.* **2020**, *167* (3), 037532.

(3) Li, D.; Duan, H.; Ma, Y.; Deng, W. Headspace-Sampling Paper-Based Analytical Device for Colorimetric/Surface-Enhanced Raman Scattering Dual Sensing of Sulfur Dioxide in Wine. *Anal. Chem.* **2018**, *90* (9), 5719−5727.

(4) Nawaz, H.; Zhang, J.; Tian, W.; Jin, K.; Jia, R.; Yang, T.; Zhang, J. Cellulose-Based Fluorescent Sensor for Visual and Versatile Detection of Amines and Anions. *J. Hazard. Mater.* **2020**, *387*, 121719.

(5) Chaiyo, S.; Mehmeti, E.; Zagar, K.; Siangproh, W.; Chailapakul, O.; Kalcher, K. Electrochemical Sensors for the Simultaneous Determination of Zinc, Cadmium and Lead Using a Nafion/Ionic Liquid/Graphene Composite Modified Screen-Printed Carbon Electrode. *Anal. Chim. Acta* **2016**, *918*, 26−34.

(6) Khoshbin, Z.; Housaindokht, M. R.; Verdian, A.; Bozorgmehr, M. R. Simultaneous Detection and Determination of Mercury (II) and Lead (II) Ions through the Achievement of Novel Functional Nucleic Acid-Based Biosensors. *Biosens. Bioelectron.* **2018**, *116* (March), 130−147.

(7) Migliorini, F. L.; Sanfelice, R. C.; Pavinatto, A.; Steffens, J.; Steffens, C.; Correa, D. S. Voltammetric Cadmium (II) Sensor Based on a Fluorine Doped Tin Oxide Electrode Modified with Polyamide 6/Chitosan Electrospun Nanofibers and Gold Nanoparticles. *Microchim. Acta* **2017**, *184*, 1077−1084.

(8) Golmohammadi, M.; Morales-Narváez, E.; Naghdi, T.; Merkoçi, A. Nanocellulose in Sensing and Biosensing. *Chem. Mater.* **2017**, *29* (13), 5426−5446.

(9) Mercante, L. A.; Scagion, V. P.; Migliorini, F. L.; Mattoso, L. H. C.; Correa, D. S. Electrospinning-Based (Bio) Sensors for Food and Agricultural Applications: A Review. *TrAC, Trends Anal. Chem.* **2017**, *91*, 91−103.

(10) Soler, M.; Estevez, M. C.; Cardenosa-Rubio, M.; Astua, A.; Lechuga, L. M. How Nanophotonic Label-Free Biosensors Can Contribute to Rapid and Massive Diagnostics of Respiratory Virus Infections: COVID-19 Case. *ACS Sensors* **2020**, *5* (9), 2663−2678.

(11) Pavinatto, A.; Mercante, L. A.; Leandro, C. S.; Mattoso, L. H. C.; Correa, D. S. Layer-by-Layer Assembled Films of Chitosan and Multi-Walled Carbon Nanotubes for the Electrochemical Detection of 17 α -Ethinylestradiol. *J. Electroanal. Chem.* **2015**, *755*, 215−220.

(12) Fan, J.; Zhang, S.; Li, F.; Shi, J. Cellulose-Based Sensors for Metal Ions Detection. *Cellulose* **2020**, *27* (10), 5477−5507.

(13) Barandun, G.; Soprani, M.; Naficy, S.; Grell, M.; Kasimatis, M.; Chiu, K. L.; Ponzoni, A.; Güder, F. Cellulose Fibers Enable Near-Zero-Cost Electrical Sensing of Water-Soluble Gases. *ACS Sensors* **2019**, *4* (6), 1662−1669.

(14) Prathapan, R.; Tabor, R. F.; Garnier, G.; Hu, J. Recent Progress in Cellulose Nanocrystal Alignment and Its Applications. *ACS Appl. Bio Mater.* **2020**, *3* (4), 1828−1844.

(15) Dufresne, A. Nanocellulose Processing Properties and Potential Applications. *Curr. For. Reports* **2019**, *5* (2), 76−89.

(16) Charreau, H.; Cavallo, E.; Foresti, M. L. Patents Involving Nanocellulose: Analysis of Their Evolution since 2010. *Carbohydr. Polym.* **2020**, *237*, 116039.

(17) Klemm, D.; Cranston, E. D.; Fischer, D.; Gama, M.; Kedzior, S. A.; Kralisch, D.; Kramer, F.; Kondo, T.; Lindström, T.; Nietzsche, S.; Petzold-Welcke, K.; Rauchfuß, F. Nanocellulose as a Natural Source for Groundbreaking Applications in Materials Science: Today's State. *Mater. Today* **2018**, *21* (7), 720−748.

(18) Kamel, R.; El-Wakil, N. A.; Dufresne, A.; Elkasabgy, N. A. Nanocellulose: From an Agricultural Waste to a Valuable Pharmaceutical Ingredient. *Int. J. Biol. Macromol.* **2020**, *163*, 1579−1590.

(19) Kalambate, P. K.; Rao, Z.; Dhanjai; Wu, J.; Shen, Y.; Boddula, R.; Huang, Y. Electrochemical (Bio) Sensors Go Green. *Biosens. Bioelectron.* **2020**, *163* (April), 112270.

(20) Zhu, Q.; Liu, S.; Sun, J.; Liu, J.; Kirubaharan, C. J.; Chen, H.; Xu, W.; Wang, Q. Stimuli-Responsive Cellulose Nanomaterials for Smart Applications. *Carbohydr. Polym.* **2020**, *235*, 115933.

(21) Arduini, F.; Cinti, S.; Caratelli, V.; Amendola, L.; Palleschi, G.; Moscone, D. Origami Multiple Paper-Based Electrochemical Biosensors for Pesticide Detection. *Biosens. Bioelectron.* **2019**, *126*, 346−354.

(22) Tayeb, P.; Tayeb, A. H. Nanocellulose Applications in Sustainable Electrochemical and Piezoelectric Systems: A Review. *Carbohydr. Polym.* **2019**, *224*, 115149.

(23) Pradhan, S.; Brooks, A. K.; Yadavalli, V. K. Nature-Derived Materials for the Fabrication of Functional Biodevices. *Mater. Today Bio* **2020**, *7* (April), 100065.

(24) Maciel, J. V.; Durigon, A. M. M.; Souza, M. M.; Quadrado, R. F. N.; Fajardo, A. R.; Dias, D. Polysaccharides Derived from Natural Sources Applied to the Development of Chemically Modified Electrodes for Environmental Applications: A Review. *Trends Environ. Anal. Chem.* **2019**, *22*, No. e00062.

(25) Zhang, Y.; Zhang, L.; Cui, K.; Ge, S.; Cheng, X.; Yan, M.; Yu, J.; Liu, H. Flexible Electronics Based on Micro/Nanostructured Paper. *Adv. Mater.* **2018**, *30* (51), 1801588.

(26) Eichhorn, S. J. Cellulose Nanowhiskers: Promising Materials for Advanced Applications. *Soft Matter* **2011**, *7* (2), 303.

(27) Asyraf, M. R. M.; Rafidah, M.; Azrina, A.; Razman, M. R. Dynamic Mechanical Behaviour of Kenaf Cellulosic Fibre Biocomposites: A Comprehensive Review on Chemical Treatments. *Cellulose* **2021**, *28* (5), 2675−2695.

(28) Pandey, A. Pharmaceutical and Biomedical Applications of Cellulose Nanofibers: A Review. *Environ. Chem. Lett.* **2021**, *19* (3), 2043−2055.

(29) Lefroy, K. S.; Murray, B. S.; Ries, M. E.; Curwen, T. D. A Natural, Cellulose-Based Microgel for Water-in-Oil Emulsions. *Food Hydrocolloids* **2021**, *113*, 106408.

(30) Cazón, P.; Vázquez, M. Bacterial Cellulose as a Biodegradable Food Packaging Material: A Review. *Food Hydrocolloids* **2021**, *113*, 106530.

(31) Du, X.; Zhang, Z.; Liu, W.; Deng, Y. Nanocellulose-Based Conductive Materials and Their Emerging Applications in Energy Devices - A Review. *Nano Energy* **2017**, *35*, 299−320.

(32) Farinas, C. S.; Marconcini, J. M.; Mattoso, L. H. C. Enzymatic Conversion of Sugarcane Lignocellulosic Biomass as a Platform for the Production of Ethanol, Enzymes and Nanocellulose. *J. Renew. Mater.* **2018**, *6* (2), 203−216.
(33) Sacui, I. A.; Nieuwendaal, R. C.; Burnett, D. J.; Stranick, S. J.; Jorfi, M.; Weder, C.; Foster, E. J.; Olsson, R. T.; Gilman, J. W. Comparison of the Properties of Cellulose Nanocrystals and Cellulose Nanofibrils Isolated from Bacteria, Tunicate, and Wood Processed Using Acid, Enzymatic, Mechanical, and Oxidative Methods. *ACS Appl. Mater. Interfaces* **2014**, *6* (9), 6127−6138.
(34) Habibi, Y.; Lucia, L. A.; Rojas, O. J. Cellulose Nanocrystals: Chemistry, Self-Assembly, and Applications. *Chem. Rev.* **2010**, *110*, 3479−3500.
(35) Heinze, T. Cellulose: Structure and Properties. In *Cellulose Chemistry and Properties: Fibers, Nanocelluloses and Advanced Materials: Advances in Polymer Science*; Rojas, O. J., Ed.; Springer, 2015; Vol. *271*, pp 1−52. DOI: 10.1007/12.
(36) Nishimura, H.; Kamiya, A.; Nagata, T.; Katahira, M.; Watanabe, T. Direct Evidence for α Ether Linkage between Lignin and Carbohydrates in Wood Cell Walls. *Sci. Rep.* **2018**, *8* (1), 6538.
(37) Moon, R. J.; Martini, A.; Nairn, J.; Simonsen, J.; Youngblood, J. *Chem. Soc. Rev.* **2011**, *40*, 3941.
(38) Kose, O.; Tran, A.; Lewis, L.; Hamad, W. Y.; MacLachlan, M. J. Unwinding a Spiral of Cellulose Nanocrystals for Stimuli-Responsive Stretchable Optics. *Nat. Commun.* **2019**, *10* (1), 510.
(39) Cheng, Z.; Ye, H.; Cheng, F.; Li, H.; Ma, Y.; Zhang, Q.; Natan, A.; Mukhopadhyay, A.; Jiao, Y.; Li, Y.; Liu, Y.; Zhu, H. Tuning Chiral Nematic Pitch of Bioresourced Photonic Films via Coupling Organic Acid Hydrolysis. *Adv. Mater. Interfaces* **2019**, *6* (7), 1802010.
(40) Klemm, D.; Heublein, B.; Fink, H. P.; Bohn, A. Cellulose: Fascinating Biopolymer and Sustainable Raw Material. *Angew. Chem., Int. Ed.* **2005**, *44* (22), 3358−3393.
(41) Roy, D.; Semsarilar, M.; Guthrie, J. T.; Perrier, S. Cellulose Modification by Polymer Grafting: A Review. *Chem. Soc. Rev.* **2009**, *38* (7), 2046−2064.
(42) de Amorim, J. D. P.; de Souza, K. C.; Duarte, C. R.; da Silva Duarte, I.; de Assis Sales Ribeiro, F.; Silva, G. S.; de Farias, P. M. A.; Stingl, A.; Costa, A. F. S.; Vinhas, G. M.; Sarubbo, L. A. Plant and Bacterial Nanocellulose: Production, Properties and Applications in Medicine, Food, Cosmetics, Electronics and Engineering. A Review. *Environ. Chem. Lett.* **2020**, *18* (3), 851−869.
(43) Foster, E. J.; Moon, R. J.; Agarwal, U. P.; Bortner, M. J.; Bras, J.; Camarero-Espinosa, S.; Chan, K. J.; Clift, M. J. D.; Cranston, E. D.; Eichhorn, S. J.; Fox, D. M.; Hamad, W. Y.; Heux, L.; Jean, B.; Korey, M.; Nieh, W.; Ong, K. J.; Reid, M. S.; Renneckar, S.; Roberts, R.; Shatkin, J. A.; Simonsen, J.; Stinson-Bagby, K.; Wanasekara, N.; Youngblood, J. Current Characterization Methods for Cellulose Nanomaterials. *Chem. Soc. Rev.* **2018**, *47* (8), 2609−2679.
(44) Zhang, H.; Dou, C.; Pal, L.; Hubbe, M. A. Review of Electrically Conductive Composites and Films Containing Cellulosic Fibers or Nanocellulose. *BioResources* **2019**, *14* (3), 7494−7542.
(45) Teodoro, K. B. R.; Migliorini, F. L.; Facure, M. H. M.; Correa, D. S. Conductive Electrospun Nanofibers Containing Cellulose Nanowhiskers and Reduced Graphene Oxide for the Electrochemical Detection of Mercury(II). *Carbohydr. Polym.* **2019**, *207*, 747−754.
(46) Teodoro, K. B. R.; Shimizu, F. M.; Scagion, V. P.; Correa, D. S. Ternary Nanocomposites Based on Cellulose Nanowhiskers, Silver Nanoparticles and Electrospun Nanofibers: Use in an Electronic Tongue for Heavy Metal Detection. *Sens. Actuators, B* **2019**, *290*, 387−395.
(47) Teodoro, K. B. R.; Migliorini, F. L.; Christinelli, W. A.; Correa, D. S. Detection of Hydrogen Peroxide (H 2 O 2) Using a Colorimetric Sensor Based on Cellulose Nanowhiskers and Silver Nanoparticles. *Carbohydr. Polym.* **2019**, *212*, 235−241.
(48) *ISO/TS 20477:2017 - Nanotechnologies - Standard Terms and Their Definition for Cellulose Nanomaterial*. https://www.iso.org/standard/68153.html.
(49) Iguchi, M.; Yamanaka, S.; Budhiono, A. Bacterial Cellulose - a Masterpiece of Nature's Arts. *J. Mater. Sci.* **2000**, *35* (2), 261−270.
(50) Roman, M.; Winter, W. T. Effect of Sulfate Groups from Sulfuric Acid Hydrolysis on the Thermal Degradation Behaviour of Bacterial Cellulose. *Biomacromolecules* **2004**, *5* (5), 1671−1677.
(51) Siqueira, G.; Bras, J.; Dufresne, A. Cellulose Whiskers versus Microfibrils: Influence of the Nature of the Nanoparticle and Its Surface Functionalization on the Thermal and Mechanical Properties of Nanocomposites. *Biomacromolecules* **2009**, *10* (2), 425−432.
(52) Thomas, B.; Raj, M. C.; Athira, B. K.; Rubiyah, H. M.; Joy, J.; Moores, A.; Drisko, G. L.; Sanchez, C. Nanocellulose, a Versatile Green Platform: From Biosources to Materials and Their Applications. *Chem. Rev.* **2018**, *118* (24), 11575−11625.
(53) de Morais Teixeira, E.; Correa, A. C.; Manzoli, A.; de Lima Leite, F.; de Oliveira, C. R.; Mattoso, L. H. C. Cellulose Nanofibers from White and Naturally Colored Cotton Fibers. *Cellulose* **2010**, *17* (3), 595−606.
(54) Hubbe, M. A.; Rojas, O. J.; Lucia, L. A.; Sain, M. Cellulosic Nanocomposites: A Review. *BioResources* **2008**, *3* (3), 929−980.
(55) Bondeson, D.; Mathew, A.; Oksman, K. Optimization of the Isolation of Nanocrystals from Microcrystalline Cellulose by Acid Hydrolysis. *Cellulose* **2006**, *13* (2), 171−180.
(56) Shankar, S.; Rhim, J. W. Preparation of Nanocellulose from Micro-Crystalline Cellulose: The Effect on the Performance and Properties of Agar-Based Composite Films. *Carbohydr. Polym.* **2016**, *135*, 18−26.
(57) Buffiere, J.; Balogh-Michels, Z.; Borrega, M.; Geiger, T.; Zimmermann, T.; Sixta, H. The Chemical-Free Production of Nanocelluloses from Microcrystalline Cellulose and Their Use as Pickering Emulsion Stabilizer. *Carbohydr. Polym.* **2017**, *178*, 48−56.
(58) Neubauerova, K.; Carneiro, M. C. C. G.; Rodrigues, L. R.; Moreira, F. T. C.; Sales, M. G. F. Nanocellulose- Based Biosensor for Colorimetric Detection of Glucose. *Sens. Bio-Sensing Res.* **2020**, *29* (April), 100368.
(59) Kim, J.; Lee, D.; Lee, Y.; Chen, W.; Lee, S. Nanocellulose for Energy Storage Systems: Beyond the Limits of Synthetic Materials. *Adv. Mater.* **2019**, *31* (20), 1804826.
(60) Otoni, C. G.; Figueiredo, J. S. L.; Capeletti, L. B.; Cardoso, M. B.; Bernardes, J. S.; Loh, W. Tailoring the Antimicrobial Response of Cationic Nanocellulose-Based Foams through Cryo-Templating. *ACS Appl. Bio Mater.* **2019**, *2* (5), 1975−1986.
(61) De France, K. J.; Hoare, T.; Cranston, E. D. Review of Hydrogels and Aerogels Containing Nanocellulose. *Chem. Mater.* **2017**, *29* (11), 4609−4631.
(62) Ullah, A.; Saito, Y.; Ullah, S.; Haider, M. K.; Nawaz, H.; Duy-Nam, P.; Kharaghani, D.; Kim, I. S. Bioactive Sambong Oil-Loaded Electrospun Cellulose Acetate Nanofibers: Preparation, Characterization, and in-Vitro Biocompatibility. *Int. J. Biol. Macromol.* **2021**, *166*, 1009−1021.
(63) Hashmi, M.; Ullah, S.; Ullah, A.; Saito, Y.; Haider, M. K.; Bie, X.; Wada, K.; Kim, I. S. Carboxymethyl Cellulose (CMC) Based Electrospun Composite Nanofiber Mats for Food Packaging. *Polymers (Basel, Switz.)* **2021**, *13* (2), 302.
(64) Vocht, M. P.; Beyer, R.; Thomasic, P.; Müller, A.; Ota, A.; Hermanutz, F.; Buchmeiser, M. R. High-Performance Cellulosic Filament Fibers Prepared via Dry-Jet Wet Spinning from Ionic Liquids. *Cellulose* **2021**, *28* (5), 3055−3067.
(65) dos Santos, D. M.; Correa, D. S.; Medeiros, E. S.; Oliveira, J. E.; Mattoso, L. H. C. Advances in Functional Polymer Nanofibers: From Spinning Fabrication Techniques to Recent Biomedical Applications. *ACS Appl. Mater. Interfaces* **2020**, *12* (41), 45673−45701.
(66) Yarin, A. L. Coaxial Electrospinning and Emulsion Electrospinning of Core-Shell Fibers. *Polym. Adv. Technol.* **2011**, *22* (3), 310−317.
(67) Jiang, F.; Hsieh, Y. Lo Dual Wet and Dry Resilient Cellulose II Fibrous Aerogel for Hydrocarbon-Water Separation and Energy Storage Applications. *ACS Omega* **2018**, *3* (3), 3530−3539.
(68) Liu, H.; Hsieh, Y. Lo Ultrafine Fibrous Cellulose Membranes from Electrospinning of Cellulose Acetate. *J. Polym. Sci., Part B: Polym. Phys.* **2002**, *40* (18), 2119−2129.

(69) Frey, M. W. Electrospinning Cellulose and Cellulose Derivatives. *Polym. Rev.* **2008**, *48* (2), 378−391.
(70) Ramires, E. C.; Megiatto, J. D.; Dufresne, A.; Frollini, E. Cellulose Nanocrystals versus Microcrystalline Cellulose as Reinforcement of Lignopolyurethane Matrix. *Fibers* **2020**, *8* (4), 21.
(71) Jonoobi, M.; Oladi, R.; Davoudpour, Y.; Oksman, K.; Dufresne, A.; Hamzeh, Y.; Davoodi, R. Different Preparation Methods and Properties of Nanostructured Cellulose from Various Natural Resources and Residues: A Review. *Cellulose* **2015**, *22* (2), 935−969.
(72) Tingaut, P.; Zimmermann, T.; Sèbe, G. Cellulose Nanocrystals and Microfibrillated Cellulose as Building Blocks for the Design of Hierarchical Functional Materials. *J. Mater. Chem.* **2012**, *22* (38), 20105.
(73) Zhao, D.; Zhu, Y.; Cheng, W.; Chen, W.; Wu, Y.; Yu, H. Cellulose-Based Flexible Functional Materials for Emerging Intelligent Electronics. *Adv. Mater.* **2020**, *2000619*, 2000619.
(74) Zhu, H.; Luo, W.; Ciesielski, P. N.; Fang, Z.; Zhu, J. Y.; Henriksson, G.; Himmel, M. E.; Hu, L. Wood-Derived Materials for Green Electronics, Biological Devices, and Energy Applications. *Chem. Rev.* **2016**, *116* (16), 9305−9374.
(75) Pourreza, N.; Golmohammadi, H.; Naghdi, T.; Yousefi, H. Green In-Situ Synthesized Silver Nanoparticles Embedded in Bacterial Cellulose Nanopaper as a Bionanocomposite Plasmonic Sensor. *Biosens. Bioelectron.* **2015**, *74*, 353−359.
(76) Abeer, M. M.; Mohd Amin, M. C. I.; Martin, C. A Review of Bacterial Cellulose-Based Drug Delivery Systems: Their Biochemistry, Current Approaches and Future Prospects. *J. Pharm. Pharmacol.* **2014**, *66* (8), 1047−1061.
(77) Gullo, M.; Sola, A.; Zanichelli, G.; Montorsi, M.; Messori, M.; Giudici, P. Increased Production of Bacterial Cellulose as Starting Point for Scaled-up Applications. *Appl. Microbiol. Biotechnol.* **2017**, *101* (22), 8115−8127.
(78) Gomes, N. O.; Carrilho, E.; Machado, S. A. S.; Sgobbi, L. F. Bacterial Cellulose-Based Electrochemical Sensing Platform: A Smart Material for Miniaturized Biosensors. *Electrochim. Acta* **2020**, *349*, 136341.
(79) Huang, J.; Zhao, M.; Cai, Y.; Zimniewska, M.; Li, D.; Wei, Q. A Dual-Mode Wearable Sensor Based on Bacterial Cellulose Reinforced Hydrogels for Highly Sensitive Strain/Pressure Sensing. *Adv. Electron. Mater.* **2020**, *6* (1), 1900934.
(80) Silva, R. R.; Raymundo-Pereira, P. A.; Campos, A. M.; Wilson, D.; Otoni, C. G.; Barud, H. S.; Costa, C. A. R.; Domeneguetti, R. R.; Balogh, D. T.; Ribeiro, S. J. L.; Oliveira, O. N., Jr Microbial Nanocellulose Adherent to Human Skin Used in Electrochemical Sensors to Detect Metal Ions and Biomarkers in Sweat. *Talanta* **2020**, *218* (May), 121153.
(81) Singhsa, P.; Narain, R.; Manuspiya, H. Bacterial Cellulose Nanocrystals (BCNC) Preparation and Characterization from Three Bacterial Cellulose Sources and Development of Functionalized BCNCs as Nucleic Acid Delivery Systems. *ACS Appl. Nano Mater.* **2018**, *1* (1), 209−221.
(82) Bilatto, S.; Marconcini, J. M.; Mattoso, L. H. C.; Farinas, C. S. Lignocellulose Nanocrystals from Sugarcane Straw. *Ind. Crops Prod.* **2020**, *157*, 112938.
(83) Andree, V.; Niopek, D.; Müller, C.; Eiselt, J.-P.; Foh, N.; Rzany, A.; Hensel, B. Influence of Drying Methods on the Physical Properties of Bacterial Nanocellulose. *Mater. Res. Express* **2021**, *8* (2), 025402.
(84) Moon, S. M.; Heo, J. E.; Jeon, J.; Eom, T.; Jang, D.; Her, K.; Cho, W.; Woo, K.; Wie, J. J.; Shim, B. S. High Crystallinity of Tunicate Cellulose Nanofibers for High-Performance Engineering Films. *Carbohydr. Polym.* **2021**, *254*, 117470.
(85) Vadillo, J.; Larraza, I.; Calvo-Correas, T.; Gabilondo, N.; Derail, C.; Eceiza, A. Role of in Situ Added Cellulose Nanocrystals as Rheological Modulator of Novel Waterborne Polyurethane Urea for 3D-Printing Technology. *Cellulose* **2021**, *28* (8), 4729−4744.
(86) Lai, P. C.; Yu, S. S. Cationic Cellulose Nanocrystals-Based Nanocomposite Hydrogels: Achieving 3d Printable Capacitive Sensors with High Transparency and Mechanical Strength. *Polymers (Basel, Switz.)* **2021**, *13* (5), 688.
(87) Battirola, L. C.; Zanata, D. M.; Gonçalves, M. C. Improvement of Cellulose Acetate Dimensional Stability by Chemical Crosslinking with Cellulose Nanocrystals. *Composites, Part A* **2018**, *113*, 105−113.
(88) Zhao, Q.; Wei, Y.; Ni, C.; Wang, L.; Liu, B.; Liu, J.; Zhang, M.; Men, Y.; Sun, Z.; Xie, H.; Hu, W.; Lu, Y. Effect of Aminated Nanocrystal Cellulose on Proton Conductivity and Dimensional Stability of Proton Exchange Membranes. *Appl. Surf. Sci.* **2019**, *466*, 691−702.
(89) Operamolla, A. Recent Advances on Renewable and Biodegradable Cellulose Nanopaper Substrates for Transparent Light-Harvesting Devices: Interaction with Humid Environment. *Int. J. Photoenergy* **2019**, *2019*, 1−16.
(90) Zhu, M.; Wang, Y.; Zhu, S.; Xu, L.; Jia, C.; Dai, J.; Song, J.; Yao, Y.; Wang, Y.; Li, Y.; Henderson, D.; Luo, W.; Li, H.; Minus, M. L.; Li, T.; Hu, L. Anisotropic, Transparent Films with Aligned Cellulose Nanofibers. *Adv. Mater.* **2017**, *29* (21), 1606284.
(91) Song, W.; Lee, J. K.; Gong, M. S.; Heo, K.; Chung, W. J.; Lee, B. Y. Cellulose Nanocrystal-Based Colored Thin Films for Colorimetric Detection of Aldehyde Gases. *ACS Appl. Mater. Interfaces* **2018**, *10* (12), 10353−10361.
(92) Wu, B.; Zhu, G.; Dufresne, A.; Lin, N. Fluorescent Aerogels Based on Chemical Crosslinking between Nanocellulose and Carbon Dots for Optical Sensor. *ACS Appl. Mater. Interfaces* **2019**, *11* (17), 16048−16058.
(93) Neubauerova, K.; Carneiro, M. C. C. G.; Rodrigues, L. R.; Moreira, F. T. C.; Sales, M. G. F. Nanocellulose- Based Biosensor for Colorimetric Detection of Glucose. *Sens. Bio-Sensing Res.* **2020**, *29* (April), 100368.
(94) de Oliveira Barud, H. G.; da Silva, R. R.; Borges, M. A. C.; Castro, G. R.; Ribeiro, S. J. L.; da Silva Barud, H. Bacterial Nanocellulose in Dentistry: Perspectives and Challenges. *Molecules* **2021**, *26* (1), 49.
(95) Arduini, F.; Micheli, L.; Scognamiglio, V.; Mazzaracchio, V.; Moscone, D. Sustainable Materials for the Design of Forefront Printed (Bio)Sensors Applied in Agrifood Sector. *TrAC, Trends Anal. Chem.* **2020**, *128*, 115909.
(96) Revol, J. F.; Godbout, L.; Dong, X. M.; Gray, D. G.; Chanzy, H.; Maret, G. Chiral Nematic Suspensions of Cellulose Crystallites; Phase Separation and Magnetic Field Orientation. *Liq. Cryst.* **1994**, *16* (1), 127−134.
(97) Revol, J. F.; Bradford, H.; Giasson, J.; Marchessault, R. H.; Gray, D. G. Helicoidal Self-Ordering of Cellulose Microfibrils in Aqueous Suspension. *Int. J. Biol. Macromol.* **1992**, *14* (3), 170−172.
(98) Meng, Q.; Wang, T. J. Mechanics of Strong and Tough Cellulose Nanopaper. *Appl. Mech. Rev.* **2019**, *71* (4), 1−30.
(99) Dufresne, A.; Cavaille, J.-Y.; Vignon, M. R. Mechanical Behavior of Sheets Prepared from Sugar Beet Cellulose Microfibrils. *J. Appl. Polym. Sci.* **1997**, *64* (6), 1185−1194.
(100) Taniguchi, T.; Okamura, K. New Films Produced from Microfibrillated Natural Fibres. *Polym. Int.* **1998**, *47* (3), 291−294.
(101) Henriksson, M.; Berglund, L. A.; Isaksson, P.; Lindström, T.; Nishino, T. Cellulose Nanopaper Structures of High Toughness. *Biomacromolecules* **2008**, *9* (6), 1579−1585.
(102) Morales-Narváez, E.; Golmohammadi, H.; Naghdi, T.; Yousefi, H.; Kostiv, U.; Horák, D.; Pourreza, N.; Merkoçi, A. Nanopaper as an Optical Sensing Platform. *ACS Nano* **2015**, *9* (7), 7296.
(103) Dutta, S.; Mandal, N.; Bandyopadhyay, D. Paper-Based α-Amylase Detector for Point-of-Care Diagnostics. *Biosens. Bioelectron.* **2016**, *78*, 447−453.
(104) Bhattacharjee, M.; Bandyopadhyay, D. Flexible Paper Touchpad for Parkinson's Hand Tremor Detection. *Sens. Actuators, A* **2019**, *294*, 164−172.
(105) Mandal, N.; Mitra, S.; Bandyopadhyay, Di Paper-Sensors for Point-of-Care Monitoring of Drinking Water Quality. *IEEE Sens. J.* **2019**, *19* (18), 7936−7941.
(106) Ratajczak, K.; Stobiecka, M. High-Performance Modified Cellulose Paper-Based Biosensors for Medical Diagnostics and Early

Cancer Screening: A Concise Review. *Carbohydr. Polym.* **2020**, *229*, 115463.
(107) Esmaeili, C.; Abdi, M.; Mathew, A.; Jonoobi, M.; Oksman, K.; Rezayi, M. Synergy Effect of Nanocrystalline Cellulose for the Biosensing Detection of Glucose. *Sensors* **2015**, *15* (10), 24681−24697.
(108) Incani, V.; Danumah, C.; Boluk, Y. Nanocomposites of Nanocrystalline Cellulose for Enzyme Immobilization. *Cellulose* **2013**, *20* (1), 191−200.
(109) Zhang, X.; Shen, G.; Sun, S.; Shen, Y.; Zhang, C.; Xiao, A. Direct Immobilization of Antibodies on Dialdehyde Cellulose Film for Convenient Construction of an Electrochemical Immunosensor. *Sens. Actuators, B* **2014**, *200*, 304−309.
(110) Migliorini, F. L.; Teodoro, K. B. R.; Correa, D. S. Green-Synthesized Gold Nanoparticles Supported on Cellulose Nanowhiskers for Easy-to-Interpret Colorimetric Detection of Cadmium (II). *Cellul. Chem. Technol.* **2020**, *54* (5−6), 407−411.
(111) Zhang, L.; Lyu, S.; Zhang, Q.; Wu, Y.; Melcher, C.; Chmely, S. C.; Chen, Z.; Wang, S. Dual-Emitting Film with Cellulose Nanocrystal-Assisted Carbon Dots Grafted SrAl2O4, Eu2+, Dy3+ Phosphors for Temperature Sensing. *Carbohydr. Polym.* **2019**, *206*, 767−777.
(112) Ivanova, A.; Frka-Petesic, B.; Paul, A.; Wagner, T.; Jumabekov, A. N.; Vilk, Y.; Weber, J.; Schmedt auf der Günne, J.; Vignolini, S.; Tiemann, M.; Fattakhova-Rohlfing, D.; Bein, T. Cellulose Nanocrystal-Templated Tin Dioxide Thin Films for Gas Sensing. *ACS Appl. Mater. Interfaces* **2020**, *12* (11), 12639−12647.
(113) Wan Khalid, W. E. F.; Mat Arip, M. N.; Jasmani, L.; Lee, Y. H. A New Sensor for Methyl Paraben Using an Electrode Made of a Cellulose Nanocrystal-Reduced Graphene Oxide Nanocomposite. *Sensors* **2019**, *19* (12), 2726.
(114) Cheng, H.; Du, Y.; Wang, B.; Mao, Z.; Xu, H.; Zhang, L.; Zhong, Y.; Jiang, W.; Wang, L.; Sui, X. Flexible Cellulose-Based Thermoelectric Sponge towards Wearable Pressure Sensor and Energy Harvesting. *Chem. Eng. J.* **2018**, *338*, 1−7.
(115) Abdi, M. M.; Razalli, R. L.; Tahir, P. M.; Chaibakhsh, N.; Hassani, M.; Mir, M. Optimized Fabrication of Newly Cholesterol Biosensor Based on Nanocellulose. *Int. J. Biol. Macromol.* **2019**, *126*, 1213−1222.
(116) Uddin, K. M. A.; Jokinen, V.; Jahangiri, F.; Franssila, S.; Rojas, O. J.; Tuukkanen, S. Disposable Microfluidic Sensor Based on Nanocellulose for Glucose Detection. *Glob. Challenges* **2019**, *3* (2), 1800079.
(117) Xiong, R.; Hu, K.; Grant, A. M.; Ma, R.; Xu, W.; Lu, C.; Zhang, X.; Tsukruk, V. V. Ultrarobust Transparent Cellulose Nanocrystal-Graphene Membranes with High Electrical Conductivity. *Adv. Mater.* **2016**, *28*, 1501−1509.
(118) Kafy, A.; Akther, A.; Shishir, M. I. R.; Kim, H. C.; Yun, Y.; Kim, J. Cellulose Nanocrystal/Graphene Oxide Composite Film as Humidity Sensor. *Sens. Actuators, A* **2016**, *247*, 221−226.
(119) Pohanka, M. The Piezoelectric Biosensors: Principles and Applications, a Review. *Int. J. Electrochem. Sci.* **2017**, *12* (1), 496−506.
(120) Liu, H.; Zhong, J.; Lee, C.; Lee, S.-W.; Lin, L. A Comprehensive Review on Piezoelectric Energy Harvesting Technology: Materials, Mechanisms, and Applications. *Appl. Phys. Rev.* **2018**, *5* (4), 41306.
(121) Fukada, E. Piezoelectricity as a Fundamental Property of Wood. *Wood Sci. Technol.* **1968**, *2* (4), 299−307.
(122) Fukada, E. Piezoelectricity of Wood. *J. Phys. Soc. Jpn.* **1955**, *10* (2), 149−154.
(123) Kim, J.; Yun, S.; Ounaies, Z. Discovery of Cellulose as a Smart Material. *Macromolecules* **2006**, *39* (12), 4202−4206.
(124) Csoka, L.; Hoeger, I. C.; Rojas, O. J.; Peszlen, I.; Pawlak, J. J.; Peralta, P. N. Piezoelectric Effect of Cellulose Nanocrystals Thin Films. *ACS Macro Lett.* **2012**, *1* (7), 867−870.
(125) Khan, A.; Abas, Z.; Kim, H. S.; Kim, J. Recent Progress on Cellulose-Based Electro-Active Paper, Its Hybrid Nanocomposites and Applications. *Sensors* **2016**, *16* (8), 1172.
(126) Tadepalli, S.; Slocik, J. M.; Gupta, M. K.; Naik, R. R.; Singamaneni, S. Bio-Optics and Bio-Inspired Optical Materials. *Chem. Rev.* **2017**, *117* (20), 12705−12763.
(127) Fenzl, C.; Hirsch, T.; Wolfbeis, O. S. Photonic Crystals for Chemical Sensing and Biosensing. *Angew. Chem., Int. Ed.* **2014**, *53* (13), 3318−3335.
(128) Zhao, Y.; Gao, G.; Liu, D.; Tian, D.; Zhu, Y.; Chang, Y. Vapor Sensing with Color-Tunable Multilayered Coatings of Cellulose Nanocrystals. *Carbohydr. Polym.* **2017**, *174*, 39−47.
(129) Kim, H. N.; Ren, W. X.; Kim, J. S.; Yoon, J. Fluorescent and Colorimetric Sensors for Detection of Lead, Cadmium, and Mercury Ions. *Chem. Soc. Rev.* **2012**, *41* (8), 3210−3244.
(130) Andre, R. S.; Sanfelice, R. C.; Pavinatto, A.; Mattoso, L. H. C.; Correa, D. S. Hybrid Nanomaterials Designed for Volatile Organic Compounds Sensors: A Review. *Mater. Des.* **2018**, *156*, 154−166.
(131) Zhang, X.; Yin, J.; Yoon, J. Recent Advances in Development of Chiral Fluorescent and Colorimetric Sensors. *Chem. Rev.* **2014**, *114* (9), 4918−4959.
(132) Lu, T.; Pan, H.; Ma, J.; Li, Y.; Bokhari, S. W.; Jiang, X.; Zhu, S.; Zhang, D. Cellulose Nanocrystals/Polyacrylamide Composites of High Sensitivity and Cycling Performance to Gauge Humidity. *ACS Appl. Mater. Interfaces* **2017**, *9* (21), 18231−18237.
(133) Xu, M.; Li, W.; Ma, C.; Yu, H.; Wu, Y.; Wang, Y.; Chen, Z.; Li, J.; Liu, S. Multifunctional Chiral Nematic Cellulose Nanocrystals/Glycerol Structural Colored Nanocomposites for Intelligent Responsive Films, Photonic Inks and Iridescent Coatings. *J. Mater. Chem. C* **2018**, *6* (20), 5391−5400.
(134) He, Y. D.; Zhang, Z. L.; Xue, J.; Wang, X. H.; Song, F.; Wang, X. L.; Zhu, L. L.; Wang, Y. Z. Biomimetic Optical Cellulose Nanocrystal Films with Controllable Iridescent Color and Environmental Stimuli-Responsive Chromism. *ACS Appl. Mater. Interfaces* **2018**, *10* (6), 5805−5811.
(135) Bumbudsanpharoke, N.; Kwon, S.; Lee, W.; Ko, S. Optical Response of Photonic Cellulose Nanocrystal Film for a Novel Humidity Indicator. *Int. J. Biol. Macromol.* **2019**, *140*, 91−97.
(136) Yao, K.; Meng, Q.; Bulone, V.; Zhou, Q. Flexible and Responsive Chiral Nematic Cellulose Nanocrystal/Poly(Ethylene Glycol) Composite Films with Uniform and Tunable Structural Color. *Adv. Mater.* **2017**, *29* (28), 1701323.
(137) Wan, H.; Li, X.; Zhang, L.; Li, X.; Liu, P.; Jiang, Z.; Yu, Z. Z. Rapidly Responsive and Flexible Chiral Nematic Cellulose Nanocrystal Composites as Multifunctional Rewritable Photonic Papers with Eco-Friendly Inks. *ACS Appl. Mater. Interfaces* **2018**, *10* (6), 5918−5925.
(138) Boott, C. E.; Tran, A.; Hamad, W. Y.; MacLachlan, M. J. Cellulose Nanocrystal Elastomers with Reversible Visible Color. *Angew. Chem., Int. Ed.* **2020**, *59* (1), 226−231.
(139) Sun, Y.; Fan, W.; Zou, C.; Wei, L.; Liu, J.; Xu, Y. Ternary Supramolecular Ensembles of Cellulose Nanocrystals Exhibiting Multiscale Deformation and Mechano/Chemoresponsive Selective Reflection of Circularly Polarized Light. *ACS Sustainable Chem. Eng.* **2019**, *7* (7), 6851−6858.
(140) Hiratani, T.; Kose, O.; Hamad, W. Y.; Maclachlan, M. J. Stable and Sensitive Stimuli-Responsive Anisotropic Hydrogels for Sensing Ionic Strength and Pressure. *Mater. Horiz.* **2018**, *5* (6), 1076−1081.
(141) Gao, Y.; Jin, Z. Iridescent Chiral Nematic Cellulose Nanocrystal/Polyvinylpyrrolidone Nanocomposite Films for Distinguishing Similar Organic Solvents. *ACS Sustainable Chem. Eng.* **2018**, *6* (5), 6192−6202.
(142) Yang, H.; Choi, S. E.; Kim, D.; Park, D.; Lee, D.; Choi, S.; Nam, Y. S.; Kim, J. W. Color-Spectrum-Broadened Ductile Cellulose Films for Vapor-PH-Responsive Colorimetric Sensors. *J. Ind. Eng. Chem.* **2019**, *80*, 590−596.
(143) Yan, D.; Li, R.; Lu, W.; Piao, C.; Qiu, L.; Meng, Z.; Wang, S. Flexible Construction of Cellulose Photonic Crystal Optical Sensing Nano-Materials Detecting Organic Solvents. *Analyst* **2019**, *144* (6), 1892−1897.
(144) Dai, S.; Prempeh, N.; Liu, D.; Fan, Y.; Gu, M.; Chang, Y. Cholesteric Film of Cu(II)-Doped Cellulose Nanocrystals for

Colorimetric Sensing of Ammonia Gas. *Carbohydr. Polym.* **2017**, *174*, 531−539.
(145) Ling, Z.; Xu, F.; Edwards, J. V.; Prevost, N. T.; Nam, S.; Condon, B. D.; French, A. D. Nanocellulose as a Colorimetric Biosensor for Effective and Facile Detection of Human Neutrophil Elastase. *Carbohydr. Polym.* **2019**, *216* (April), 360−368.
(146) Naghdi, T.; Golmohammadi, H.; Vosough, M.; Atashi, M.; Saeedi, I.; Maghsoudi, M. T. Lab-on-Nanopaper: An Optical Sensing Bioplatform Based on Curcumin Embedded in Bacterial Nanocellulose as an Albumin Assay Kit. *Anal. Chim. Acta* **2019**, *1070*, 104−111.
(147) Guo, J.; Liu, D.; Filpponen, I.; Johansson, L. S.; Malho, J. M.; Quraishi, S.; Liebner, F.; Santos, H. A.; Rojas, O. J. Photoluminescent Hybrids of Cellulose Nanocrystals and Carbon Quantum Dots as Cytocompatible Probes for in Vitro Bioimaging. *Biomacromolecules* **2017**, *18* (7), 2045−2055.
(148) Santos, M. V.; Tercjak, A.; Gutierrez, J.; Barud, H. S.; Napoli, M.; Nalin, M.; Ribeiro, S. J. L. Optical Sensor Platform Based on Cellulose Nanocrystals (CNC) - 4′-(Hexyloxy)-4-Biphenylcarbonitrile (HOBC) Bi-Phase Nematic Liquid Crystal Composite Films. *Carbohydr. Polym.* **2017**, *168*, 346−355.
(149) Faham, S.; Golmohammadi, H.; Ghavami, R.; Khayatian, G. A Nanocellulose-Based Colorimetric Assay Kit for Smartphone Sensing of Iron and Iron-Chelating Deferoxamine Drug in Biofluids. *Anal. Chim. Acta* **2019**, *1087*, 104−112.
(150) Wu, J.; Feng, Y.; Zhang, L.; Wu, W. Nanocellulose-Based Surface-Enhanced Raman Spectroscopy Sensor for Highly Sensitive Detection of TNT. *Carbohydr. Polym.* **2020**, *248* (July), 116766.
(151) Ogundare, S. A.; van Zyl, W. E. Amplification of SERS "Hot Spots" by Silica Clustering in a Silver-Nanoparticle/Nanocrystalline-Cellulose Sensor Applied in Malachite Green Detection. *Colloids Surf., A* **2019**, *570*, 156−164.
(152) Tran, A.; Boott, C. E.; MacLachlan, M. J. Understanding the Self-Assembly of Cellulose Nanocrystals—Toward Chiral Photonic Materials. *Adv. Mater.* **2020**, *32* (41), 1905876.
(153) Zhang, Y. P.; Chodavarapu, V. P.; Kirk, A. G.; Andrews, M. P. Structured Color Humidity Indicator from Reversible Pitch Tuning in Self-Assembled Nanocrystalline Cellulose Films. *Sens. Actuators, B* **2013**, *176*, 692−697.
(154) Bumbudsanpharoke, N.; Lee, W.; Chung, U.; Ko, S. Study of Humidity-Responsive Behavior in Chiral Nematic Cellulose Nanocrystal Films for Colorimetric Response. *Cellulose* **2018**, *25* (1), 305−317.
(155) Cachelin, P.; Green, J. P.; Peijs, T.; Heeney, M.; Bastiaansen, C. W. M. Optical Acetone Vapor Sensors Based on Chiral Nematic Liquid Crystals and Reactive Chiral Dopants. *Adv. Opt. Mater.* **2016**, *4* (4), 592−596.
(156) Fiorati, A.; Bellingeri, A.; Punta, C.; Corsi, I.; Venditti, I. Silver Nanoparticles Forwater Pollution Monitoring and Treatments: Ecosafety Challenge and Cellulose-Based Hybrids Solution. *Polymers (Basel, Switz.)* **2020**, *12* (8). 1635.
(157) Purwidyantri, A.; Karina, M.; Hsu, C.-H.; Srikandace, Y.; Prabowo, B. A.; Lai, C.-S. Facile Bacterial Cellulose Nanofibrillation for the Development of a Plasmonic Paper Sensor. *ACS Biomater. Sci. Eng.* **2020**, *6* (5), 3122−3131.
(158) Nabeela, K.; Thomas, R. T.; Mohamed, A. P.; Pillai, S. Nanocellulose-Silver Ensembles for Ultrasensitive SERS: An Investigation on the Role of Nanocellulose Fibers in the Generation of High-Density Hotspots. *Appl. Mater. Today* **2020**, *20*, 100672.
(159) Xia, Z.; Li, D.; Deng, W. Identification and Detection of Volatile Aldehydes as Lung Cancer Biomarkers by Vapor Generation Combined with Paper-Based Thin-Film Microextraction. *Anal. Chem.* **2021**, *93* (11), 4924−4931.
(160) Li, D.; Ma, Y.; Duan, H.; Deng, W.; Li, D. Griess Reaction-Based Paper Strip for Colorimetric/Fluorescent/SERS Triple Sensing of Nitrite. *Biosens. Bioelectron.* **2018**, *99*, 389−398.
(161) Ma, Y.; Wang, Y.; Luo, Y.; Duan, H.; Li, D.; Xu, H.; Fodjo, E. K. Rapid and Sensitive On-Site Detection of Pesticide Residues in Fruits and Vegetables Using Screen-Printed Paper-Based SERS Swabs. *Anal. Methods* **2018**, *10* (38), 4655−4664.
(162) Ruiz-Palomero, C.; Benítez-Martínez, S.; Soriano, M. L.; Valcárcel, M. Fluorescent Nanocellulosic Hydrogels Based on Graphene Quantum Dots for Sensing Laccase. *Anal. Chim. Acta* **2017**, *974*, 93−99.
(163) Teodoro, K. B. R.; Sanfelice, R. C.; Mattoso, L. H. C.; Correa, D. S. Cellulose Whiskers Influence the Morphology and Antibacterial Properties of Silver Nanoparticles Composites. *J. Nanosci. Nanotechnol.* **2018**, *18*, 4876−4883.
(164) Asnag, G. M.; Oraby, A. H.; Abdelghany, A. M. Green Synthesis of Gold Nanoparticles and Its Effect on the Optical, Thermal and Electrical Properties of Carboxymethyl Cellulose. *Composites, Part B* **2019**, *172* (May), 436−446.
(165) Collins, C. C.; Regalado-Love, S.; Portillo, R. I.; Boston, D. J.; Shores, M. P.; Bhowmick, I. Functionalized Cellulose-Co(II)-Bis-Terpyridine Hybrid Material as Colorimetric Sensor for Micromolar Aqueous Cyanide. *Adv. Mater. Technol.* **2019**, *4* (1), 1800406.
(166) Nwosu, F. O.; Saliu, O. D.; Oyinlola, K. A.; Ojo, E. O. Colorimetric Based Polysorbate Crosslinked Cellulose-Ag-Cu Nanohybrid Sensor for Urea Sensing Applications. *J. Polym. Environ.* **2020**, *28* (5), 1475−1483.
(167) Ye, X.; Kang, Y.; Zhou, J. Rhodamine Labeled Cellulose Nanocrystals as Selective "Naked-Eye" Colorimetric and Fluorescence Sensor for Hg2+ in Aqueous Solutions. *Cellulose* **2020**, *27* (9), 5197−5210.
(168) Milindanuth, P.; Pisitsak, P. A Novel Colorimetric Sensor Based on Rhodamine-B Derivative and Bacterial Cellulose for the Detection of Cu(II) Ions in Water. *Mater. Chem. Phys.* **2018**, *216*, 325−331.
(169) Tungsombatvisit, N.; Inprasit, T.; Rohmawati, D.; Pisitsak, P. Rhodamine Derivative- Based Cellulose Acetate Electrospun Colorimetric Sensor for Cu2+ Sensing in Water: Effects of Alkaline Treatment. *Fibers Polym.* **2019**, *20* (3), 481−489.
(170) Xiong, R.; Yu, S.; Smith, M. J.; Zhou, J.; Krecker, M.; Zhang, L.; Nepal, D.; Bunning, T. J.; Tsukruk, V. V. Self-Assembly of Emissive Nanocellulose/Quantum Dot Nanostructures for Chiral Fluorescent Materials. *ACS Nano* **2019**, *13* (8), 9074−9081.
(171) Chekini, M.; Prince, E.; Zhao, L.; Mundoor, H.; Smalyukh, I. I.; Kumacheva, E. Chiral Carbon Dots Synthesized on Cellulose Nanocrystals. *Adv. Opt. Mater.* **2020**, *8* (4), 1901911.
(172) Kim, J. H.; Mun, S.; Ko, H. U.; Yun, G. Y.; Kim, J. Disposable Chemical Sensors and Biosensors Made on Cellulose Paper. *Nanotechnology* **2014**, *25* (9), 092001.
(173) Taweetanavanich, T.; Wanno, B.; Tuntulani, T.; Pulpoka, B.; Kaewtong, C. A PH Optical and Fluorescent Sensor Based on Rhodamine Modified on Activated Cellulose Paper. *J. Chin. Chem. Soc.* **2019**, *66* (5), 493−499.
(174) Cerqueira, A. S.; Duque, C. A.; Trindade, R. M.; Ribeiro, M. V. Digital System for Detection and Classification of Electrical Events. In *2005 IEEE International Symposium on Circuits and Systems*; IEEE, 2005; pp 5417−5420. DOI: 10.1109/ISCAS.2005.1465861.
(175) Bard, A. J.; Faulkner, L. R. *Electrochemical Methods: Fundamentals and Applications*, 2nd ed.; Wiley: New York, 2000.
(176) Brett, C. M. A.; Brett, A. M.. *Electrochemistry- Principles, Methods and Applications*; 1994.
(177) Bandodkar, A. J.; Wang, J. Non-Invasive Wearable Electrochemical Sensors: A Review. *Trends Biotechnol.* **2014**, *32* (7), 363−371.
(178) Stradiotto, N. R.; Yamanaka, H.; Zanoni, M. V. B. Review Electrochemical Sensors: A Powerful Tool in Analytical Chemistry. *J. Braz. Chem. Soc.* **2003**, *14* (2), 159−173.
(179) Sun, Q.; Qian, B.; Uto, K.; Chen, J.; Liu, X.; Minari, T. Functional Biomaterials towards Flexible Electronics and Sensors. *Biosens. Bioelectron.* **2018**, *119*, 237−251.
(180) Chinnappan, A.; Baskar, C.; Baskar, S.; Ratheesh, G.; Ramakrishna, S. An Overview of Electrospun Nanofibers and Their Application in Energy Storage, Sensors and Wearable/Flexible Electronics. *J. Mater. Chem. C* **2017**, *5* (48), 12657−12673.

(181) Mercante, L. A.; Scagion, V. P.; Migliorini, F. L.; Mattoso, L. H. C.; Correa, D. S. Electrospinning-Based (Bio)Sensors for Food and Agricultural Applications: A Review. *TrAC, Trends Anal. Chem.* **2017**, *91*, 91−103.
(182) Su, Z.; Ding, J.; Wei, G. Electrospinning: A Facile Technique for Fabricating Polymeric Nanofibers Doped with Carbon Nanotubes and Metallic Nanoparticles for Sensor Applications. *RSC Adv.* **2014**, *4* (94), 52598−52610.
(183) Fukuzumi, H.; Saito, T.; Iwata, T.; Kumamoto, Y.; Isogai, A. Transparent and High Gas Barrier Films of Cellulose Nanofibers Prepared by TEMPO-Mediated Oxidation. *Biomacromolecules* **2009**, *10* (1), 162−165.
(184) Nogi, M.; Iwamoto, S.; Nakagaito, A. N.; Yano, H. Optically Transparent Nanofiber Paper. *Adv. Mater.* **2009**, *21* (16), 1595−1598.
(185) Dufresne, A. Nanocellulose: A New Ageless Bionanomaterial. *Mater. Today* **2013**, *16* (6), 220−227.
(186) Bi, Q.; Dong, S.; Sun, Y.; Lu, X.; Zhao, L. An Electrochemical Sensor Based on Cellulose Nanocrystal for the Enantioselective Discrimination of Chiral Amino Acids. *Anal. Biochem.* **2016**, *508*, 50−57.
(187) Klemm, D.; Kramer, F.; Moritz, S.; Lindström, T.; Ankerfors, M.; Gray, D.; Dorris, A. Nanocelluloses: A New Family of Nature-Based Materials. *Angew. Chem., Int. Ed.* **2011**, *50* (24), 5438−5466.
(188) Saito, T.; Kuramae, R.; Wohlert, J.; Berglund, L. A.; Isogai, A. An Ultrastrong Nanofibrillar Biomaterial: The Strength of Single Cellulose Nanofibrils Revealed via Sonication-Induced Fragmentation. *Biomacromolecules* **2013**, *14* (1), 248−253.
(189) Migliorini, F. L.; Teodoro, K. B. R.; Scagion, V. P.; dos Santos, D. M.; Fonseca, F. J.; Mattoso, L. H. C.; Correa, D. S. Tuning the Electrical Properties of Electrospun Nanofibers with Hybrid Nanomaterials for Detecting Isoborneol in Water Using an Electronic Tongue. *Surfaces* **2019**, *2* (2), 432−443.
(190) Annu; Sharma, S.; Nitin, A.; Jain, R. Cellulose Fabricated Pencil Graphite Sensor for the Quantification of Hazardous Herbicide Atrazine. *Diamond Relat. Mater.* **2020**, *105* (March), 107788.
(191) Jang, M.; Kim, S. K.; Lee, J.; Ji, S.; Song, W.; Myung, S.; Lim, J.; Lee, S. S.; Jung, H. K.; Lee, J.; An, K. S. Amplifying Gas Sensor Performance by Embedding a Cellulose-Based Buffer Layer in Organic Transistors. *J. Mater. Chem. C* **2019**, *7* (46), 14504−14510.
(192) Zaid, M. H. M.; Abdullah, J.; Yusof, N. A.; Wasoh, H.; Sulaiman, Y.; Noh, M. F. M.; Issa, R. Reduced Graphene Oxide/TEMPO-Nanocellulose Nanohybrid-Based Electrochemical Biosensor for the Determination of Mycobacterium Tuberculosis. *J. Sens.* **2020**, *2020*, 1.
(193) Anirudhan, T. S.; Deepa, J. R.; Binussreejayan. Electrochemical Sensing of Cholesterol by Molecularly Imprinted Polymer of Silylated Graphene Oxide and Chemically Modified Nanocellulose Polymer. *Mater. Sci. Eng., C* **2018**, *92*, 942−956.
(194) Manan, F. A. A.; Hong, W. W.; Abdullah, J.; Yusof, N. A.; Ahmad, I. Nanocrystalline Cellulose Decorated Quantum Dots Based Tyrosinase Biosensor for Phenol Determination. *Mater. Sci. Eng., C* **2019**, *99*, 37−46.
(195) Tang, Y.; Petropoulos, K.; Kurth, F.; Gao, H.; Migliorelli, D.; Guenat, O.; Generelli, S. Screen-Printed Glucose Sensors Modified with Cellulose Nanocrystals (CNCs) for Cell Culture Monitoring. *Biosensors* **2020**, *10* (9), 125.
(196) Burrs, S. L.; Bhargava, M.; Sidhu, R.; Kiernan-Lewis, J.; Gomes, C.; Claussen, J. C.; McLamore, E. S. A Paper Based Graphene-Nanocauliflower Hybrid Composite for Point of Care Biosensing. *Biosens. Bioelectron.* **2016**, *85*, 479−487.
(197) Li, G.; Sun, K.; Li, D.; Lv, P.; Wang, Q.; Huang, F.; Wei, Q. Biosensor Based on Bacterial Cellulose-Au Nanoparticles Electrode Modified with Laccase for Hydroquinone Detection. *Colloids Surf., A* **2016**, *509*, 408−414.
(198) Cho, S.-Y.; Yu, H.; Choi, J.; Kang, H.; Park, S.; Jang, J.-S.; Hong, H.-J.; Kim, I.-D.; Lee, S.-K.; Jeong, H. S.; Jung, H.-T. Continuous Meter-Scale Synthesis of Weavable Tunicate Cellulose/Carbon Nanotube Fibers for High-Performance Wearable Sensors. *ACS Nano* **2019**, *13* (8), 9332−9341.
(199) Aragay, G.; Pons, J.; Merkoi, A. Enhanced Electrochemical Detection of Heavy Metals at Heated Graphite Nanoparticle-Based Screen-Printed Electrodes. *J. Mater. Chem.* **2011**, *21* (12), 4326−4331.
(200) Elliott, B.; Muir, C.; DeCatanzaro, D. Sources of Variance within and among Young Men in Concentrations of 17β-Estradiol and Testosterone in Axillary Perspiration. *Physiol. Behav.* **2017**, *173*, 23−29.
(201) Molinero-Abad, B.; Izquierdo, D.; Pérez, L.; Escudero, I.; Arcos-Martínez, M. J. Comparison of Backing Materials of Screen Printed Electrochemical Sensors for Direct Determination of the Sub-Nanomolar Concentration of Lead in Seawater. *Talanta* **2018**, *182*, 549−557.
(202) Si, Y.; Park, J. W.; Jung, S.; Hwang, G.-S.; Goh, E.; Lee, H. J. Layer-by-Layer Electrochemical Biosensors Configuring Xanthine Oxidase and Carbon Nanotubes/Graphene Complexes for Hypoxanthine and Uric Acid in Human Serum Solutions. *Biosens. Bioelectron.* **2018**, *121*, 265−271.
(203) Zheng, C.; Yue, Y.; Gan, L.; Xu, X.; Mei, C.; Han, J. Highly Stretchable and Self-Healing Strain Sensors Based on Nanocellulose-Supported Graphene Dispersed in Electro-Conductive Hydrogels. *Nanomaterials* **2019**, *9* (7), 937.
(204) Migliorini, F. L.; dos Santos, D. M.; Soares, A. C.; Mattoso, L. H. C.; Oliveira, O. N.; Correa, D. S. Design of a Low-Cost and Disposable Paper-Based Immunosensor for the Rapid and Sensitive Detection of Aflatoxin B1. *Chemosensors* **2020**, *8* (3), 87.
(205) Braga, G. S.; Paterno, L. G.; Fonseca, F. J. Performance of an Electronic Tongue during Monitoring 2-Methylisoborneol and Geosmin in Water Samples. *Sens. Actuators, B* **2012**, *171−172*, 181−189.
(206) Giannetto, M.; Umiltà, E.; Careri, M. New Competitive Dendrimer-Based and Highly Selective Immunosensor for Determination of Atrazine in Environmental, Feed and Food Samples: The Importance of Antibody Selectivity for Discrimination among Related Triazinic Metabolites. *Anal. Chim. Acta* **2014**, *806*, 197−203.
(207) Liu, X.; Li, W. J.; Li, L.; Yang, Y.; Mao, L. G.; Peng, Z. A Label-Free Electrochemical Immunosensor Based on Gold Nanoparticles for Direct Detection of Atrazine. *Sens. Actuators, B* **2014**, *191*, 408−414.
(208) Yang, M.; Zhao, X.; Zheng, S.; Liu, X.; Jin, B.; Li, H.; Gan, Y. A New Electrochemical Platform for Ultrasensitive Detection of Atrazine Based on Modified Self-Ordered Nb2O5 Nanotube Arrays. *J. Electroanal. Chem.* **2017**, *791*, 17−22.
(209) Wang, Y.; Qu, K.; Tang, L.; Li, Z.; Moore, E.; Zeng, X.; Liu, Y.; Li, J. Nanomaterials in Carbohydrate Biosensors. *TrAC, Trends Anal. Chem.* **2014**, *58*, 54−70.
(210) Lu, X.; Sun, J.; Sun, X. Recent Advances in Biosensors for the Detection of Estrogens in the Environment and Food. *TrAC, Trends Anal. Chem.* **2020**, *127*, 115882.
(211) Zhang, W.; Asiri, A. M.; Liu, D.; Du, D.; Lin, Y. Nanomaterial-Based Biosensors for Environmental and Biological Monitoring of Organophosphorus Pesticides and Nerve Agents. *TrAC, Trends Anal. Chem.* **2014**, *54*, 1−10.
(212) Pérez-López, B.; Merkoçi, A. Nanomaterials Based Biosensors for Food Analysis Applications. *Trends Food Sci. Technol.* **2011**, *22* (11), 625−639.
(213) Wang, W.; Gunasekaran, S. Nanozymes-Based Biosensors for Food Quality and Safety. *TrAC, Trends Anal. Chem.* **2020**, *126*, 115841.
(214) Pirzada, M.; Altintas, Z. Nanomaterials for Healthcare Biosensing Applications. *Sensors* **2019**, *19* (23), 5311.
(215) Zhu, C.; Yang, G.; Li, H.; Du, D.; Lin, Y. Electrochemical Sensors and Biosensors Based on Nanomaterials and Nanostructures. *Anal. Chem.* **2015**, *87* (1), 230−249.
(216) Edwards, J. V.; Prevost, N.; French, A.; Concha, M.; Delucca, A.; Wu, Q. Nanocellulose-Based Biosensors: Design, Preparation, and Activity of Peptide-Linked Cotton Cellulose Nanocrystals Having Fluorimetric and Colorimetric Elastase Detection Sensitivity. *Engineering* **2013**, *05*, 20−28.

https://doi.org/10.1021/acssensors.1c00473
ACS Sens. 2021, 6, 2473−2496

(217) Shi, Z.; Phillips, G. O.; Yang, G. Nanocellulose Electroconductive Composites. *Nanoscale* **2013**, *5* (8), 3194−3201.
(218) Liu, C.; Dong, J.; Waterhouse, G. I. N.; Cheng, Z.; Ai, S. Electrochemical Immunosensor with Nanocellulose-Au Composite Assisted Multiple Signal Amplification for Detection of Avian Leukosis Virus Subgroup J. *Biosens. Bioelectron.* **2018**, *101*, 110−115.
(219) Arakawa, T.; Tomoto, K.; Nitta, H.; Toma, K.; Takeuchi, S.; Sekita, T.; Minakuchi, S.; Mitsubayashi, K. A Wearable Cellulose Acetate-Coated Mouthguard Biosensor for In Vivo Salivary Glucose Measurement. *Anal. Chem.* **2020**, *92* (18), 12201−12207.
(220) Lawrence, C. S. K. L.; Tan, S. N.; Floresca, C. Z. A "Green" Cellulose Paper Based Glucose Amperometric Biosensor. *Sens. Actuators, B* **2014**, *193*, 536−541.
(221) Yuan, H.; Chen, L.; Hong, F. F.; Zhu, M. Evaluation of Nanocellulose Carriers Produced by Four Different Bacterial Strains for Laccase Immobilization. *Carbohydr. Polym.* **2018**, *196*, 457−464.
(222) Wang, J.; Yiu, B.; Obermeyer, J.; Filipe, C. D. M.; Brennan, J. D.; Pelton, R. Effects of Temperature and Relative Humidity on the Stability of Paper-Immobilized Antibodies. *Biomacromolecules* **2012**, *13* (2), 559−564.
(223) Pirich, C. L.; de Freitas, R. A.; Torresi, R. M.; Picheth, G. F.; Sierakowski, M. R. Piezoelectric Immunochip Coated with Thin Films of Bacterial Cellulose Nanocrystals for Dengue Detection. *Biosens. Bioelectron.* **2017**, *92*, 47−53.
(224) Tracey, C. T.; Torlopov, M. A.; Martakov, I. S.; Vdovichenko, E. A.; Zhukov, M.; Krivoshapkin, P. V.; Mikhaylov, V. I.; Krivoshapkina, E. F. Hybrid Cellulose Nanocrystal/Magnetite Glucose Biosensors. *Carbohydr. Polym.* **2020**, *247* (June), 116704.
(225) Kamel, S.; Khattab, T. Recent Advances in Cellulose-Based Biosensors For. *Biosensors* **2020**, *10*, 67.
(226) Arakawa, T.; Kuroki, Y.; Nitta, H.; Chouhan, P.; Toma, K.; Sawada, S.; Ichi Takeuchi, S.; Sekita, T.; Akiyoshi, K.; Minakuchi, S.; Mitsubayashi, K. Mouthguard Biosensor with Telemetry System for Monitoring of Saliva Glucose: A Novel Cavitas Sensor. *Biosens. Bioelectron.* **2016**, *84*, 106−111.
(227) Islam, M. S.; Chen, L.; Sisler, J.; Tam, K. C. Cellulose Nanocrystal (CNC)-Inorganic Hybrid Systems: Synthesis, Properties and Applications. *J. Mater. Chem. B* **2018**, *6* (6), 864−883.
(228) Kafy, A.; Sadasivuni, K. K.; Akther, A.; Min, S. K.; Kim, J. Cellulose/Graphene Nanocomposite as Multifunctional Electronic and Solvent Sensor Material. *Mater. Lett.* **2015**, *159*, 20−23.
(229) Hosseini, H.; Kokabi, M.; Mousavi, S. M. Conductive Bacterial Cellulose/Multiwall Carbon Nanotubes Nanocomposite Aerogel as a Potentially Flexible Lightweight Strain Sensor. *Carbohydr. Polym.* **2018**, *201* (May), 228−235.
(230) Xie, Y.; Xu, H.; He, X.; Hu, Y.; Zhu, E.; Gao, Y.; Liu, D.; Shi, Z.; Li, J.; Yang, Q.; Xiong, C. Flexible Electronic Skin Sensor Based on Regenerated Cellulose/Carbon Nanotube Composite Films. *Cellulose* **2020**, *27* (17), 10199−10211.
(231) Lay, M.; Pèlach, M. À.; Pellicer, N.; Tarrés, J. A.; Bun, K. N.; Vilaseca, F. Smart Nanopaper Based on Cellulose Nanofibers with Hybrid PEDOT:PSS/Polypyrrole for Energy Storage Devices. *Carbohydr. Polym.* **2017**, *165*, 86−95.
(232) Luo, M.; Li, M.; Li, Y.; Chang, K.; Liu, K.; Liu, Q.; Wang, Y.; Lu, Z.; Liu, X.; Wang, D. In-Situ Polymerization of PPy/Cellulose Composite Sponge with High Elasticity and Conductivity for the Application of Pressure Sensor. *Compos. Commun.* **2017**, *6*, 68−72.
(233) Moccelini, S. K.; Franzoi, A. C.; Vieira, I. C.; Dupont, J.; Scheeren, C. W. A Novel Support for Laccase Immobilization: Cellulose Acetate Modified with Ionic Liquid and Application in Biosensor for Methyldopa Detection. *Biosens. Bioelectron.* **2011**, *26* (8), 3549−3554.
(234) Naresh, V.; Lee, N. A Review on Biosensors and Recent Development of Nanostructured Materials-Enabled Biosensors. *Sensors* **2021**, *21* (4), 1109.
(235) Habibi, Y.; Chanzy, H.; Vignon, M. R. TEMPO-Mediated Surface Oxidation of Cellulose Whiskers. *Cellulose* **2006**, *13* (6), 679−687.
(236) Li, L.; Zhao, S.; Zhang, J.; Zhang, Z. X.; Hu, H.; Xin, Z.; Kim, J. K. TEMPO-Mediated Oxidation of Microcrystalline Cellulose: Influence of Temperature and Oxidation Procedure on Yields of Water-Soluble Products and Crystal Structures of Water-Insoluble Residues. *Fibers Polym.* **2013**, *14* (3), 352−357.
(237) de Nooy, A.E.J.; Besemer, A.C.; van Bekkum, H. Highly Selective Tempo Mediated Oxidation of Primary Alcohol Groups in Polysaccharides. *Recl. des Trav. Chim. des Pays-Bas* **1994**, *113* (3), 165−166.
(238) Choi, J.; Ghaffari, R.; Baker, L. B.; Rogers, J. A. Skin-Interfaced Systems for Sweat Collection and Analytics. *Sci. Adv.* **2018**, *4* (2), eaar3921.
(239) Min, J.; Sempionatto, J. R.; Teymourian, H.; Wang, J.; Gao, W. Wearable Electrochemical Biosensors in North America. *Biosens. Bioelectron.* **2021**, *172*, 112750.
(240) Kim, J.; Campbell, A. S.; de Ávila, B. E. F.; Wang, J. Wearable Biosensors for Healthcare Monitoring. *Nat. Biotechnol.* **2019**, *37* (4), 389−406.
(241) Huang, J.; Li, D.; Zhao, M.; Ke, H.; Mensah, A.; Lv, P.; Tian, X.; Wei, Q. Flexible Electrically Conductive Biomass-Based Aerogels for Piezoresistive Pressure/Strain Sensors. *Chem. Eng. J.* **2019**, *373* (May), 1357−1366.
(242) Yan, C.; Wang, J.; Kang, W.; Cui, M.; Wang, X.; Foo, C. Y.; Chee, K. J.; Lee, P. S. Highly Stretchable Piezoresistive Graphene-Nanocellulose Nanopaper for Strain Sensors. *Adv. Mater.* **2014**, *26* (13), 2022−2027.
(243) Lemaire, E.; Moser, R.; Borsa, C. J.; Briand, D. Green Paper-Based Piezoelectronics for Sensors and Actuators. *Sens. Actuators, A* **2016**, *244*, 285−291.
(244) Tai, H.; Duan, Z.; Wang, Y.; Wang, S.; Jiang, Y. Paper-Based Sensors for Gas, Humidity, and Strain Detections: A Review. *ACS Appl. Mater. Interfaces* **2020**, *12* (28), 31037−31053.
(245) Rajala, S.; Siponkoski, T.; Sarlin, E.; Mettänen, M.; Vuoriluoto, M.; Pammo, A.; Juuti, J.; Rojas, O. J.; Franssila, S.; Tuukkanen, S. Cellulose Nanofibril Film as a Piezoelectric Sensor Material. *ACS Appl. Mater. Interfaces* **2016**, *8* (24), 15607−15614.
(246) Yun, S.; Jang, S.; Yun, G.-Y.; Kim, J. Electrically Aligned Cellulose Film for Electro-Active Paper and Its Piezoelectricity. *Smart Mater. Struct.* **2009**, *18* (11), 117001.
(247) Fashandi, H.; Abolhasani, M. M.; Sandoghdar, P.; Zohdi, N.; Li, Q.; Naebe, M. Morphological Changes towards Enhancing Piezoelectric Properties of PVDF Electrical Generators Using Cellulose Nanocrystals. *Cellulose* **2016**, *23* (6), 3625−3637.
(248) Fu, R.; Chen, S.; Lin, Y.; Zhang, S.; Jiang, J.; Li, Q.; Gu, Y. Improved Piezoelectric Properties of Electrospun Poly(Vinylidene Fluoride) Fibers Blended with Cellulose Nanocrystals. *Mater. Lett.* **2017**, *187*, 86−88.
(249) Ko, H.-U.; Kim, H. C.; Kim, J. W.; Zhai, L.; Kim, J. Fabrication Method Study of ZnO Nanocoated Cellulose Film and Its Piezoelectric Property. *Materials* **2017**, *10* (6), 611.
(250) Pusty, M.; Shirage, P. M. Gold Nanoparticle-Cellulose/PDMS Nanocomposite: A Flexible Dielectric Material for Harvesting Mechanical Energy. *RSC Adv.* **2020**, *10* (17), 10097−10112.
(251) Hänninen, A.; Sarlin, E.; Lyyra, I.; Salpavaara, T.; Kellomäki, M.; Tuukkanen, S. Nanocellulose and Chitosan Based Films as Low Cost, Green Piezoelectric Materials. *Carbohydr. Polym.* **2018**, *202*, 418−424.
(252) Ng, T. H.; Liao, W. H. Sensitivity Analysis and Energy Harvesting for a Self-Powered Piezoelectric Sensor. *J. Intell. Mater. Syst. Struct.* **2005**, *16* (10), 785−797.
(253) Sappati, K. K.; Bhadra, S. Piezoelectric Polymer and Paper Substrates: A Review. *Sensors* **2018**, *18* (11), 3605.
(254) Zhang, S.; Liu, H.; Yang, S.; Shi, X.; Zhang, D.; Shan, C.; Mi, L.; Liu, C.; Shen, C.; Guo, Z. Ultrasensitive and Highly Compressible Piezoresistive Sensor Based on Polyurethane Sponge Coated with a Cracked Cellulose Nanofibril/Silver Nanowire Layer. *ACS Appl. Mater. Interfaces* **2019**, *11* (11), 10922−10932.
(255) Yan, Q.; Xie, W.; Zhou, M.; Fu, H. An Ultrasensitive and Highly Compressive Piezoresistive Sensor Based on a Biopolyol-

https://doi.org/10.1021/acssensors.1c00473
ACS Sens. 2021, 6, 2473−2496

Reinforced Polyurethane Sponge Coated with Silver Nanoparticles and Carbon Nanotubes/Cellulose Nanocrystals. *J. Mater. Chem. C* **2020**, *8* (46), 16603−16614.
(256) Jung, M.; Kim, K.; Kim, B.; Lee, K. J.; Kang, J. W.; Jeon, S. Vertically Stacked Nanocellulose Tactile Sensor. *Nanoscale* **2017**, *9* (44), 17212−17219.
(257) Zhu, L.; Zhou, X.; Liu, Y.; Fu, Q. Highly Sensitive, Ultrastretchable Strain Sensors Prepared by Pumping Hybrid Fillers of Carbon Nanotubes/Cellulose Nanocrystal into Electrospun Polyurethane Membranes. *ACS Appl. Mater. Interfaces* **2019**, *11* (13), 12968−12977.
(258) Li, M.; Jie, Y.; Shao, L.-H.; Guo, Y.; Cao, X.; Wang, N.; Wang, Z. L. All-in-One Cellulose Based Hybrid Tribo/Piezoelectric Nanogenerator. *Nano Res.* **2019**, *12* (8), 1831−1835.
(259) Zhang, S.; Sun, K.; Liu, H.; Chen, X.; Zheng, Y.; Shi, X.; Zhang, D.; Mi, L.; Liu, C.; Shen, C. Enhanced Piezoresistive Performance of Conductive WPU/CNT Composite Foam through Incorporating Brittle Cellulose Nanocrystal. *Chem. Eng. J.* **2020**, *387*, 124045.
(260) Guan, F.; Xie, Y.; Wu, H.; Meng, Y.; Shi, Y.; Gao, M.; Zhang, Z.; Chen, S.; Chen, Y.; Wang, H.; Pei, Q. Silver Nanowire-Bacterial Cellulose Composite Fiber-Based Sensor for Highly Sensitive Detection of Pressure and Proximity. *ACS Nano* **2020**, *14* (11), 15428−15439.
(261) Hu, W.; Chen, S.; Zhou, B.; Liu, L.; Ding, B.; Wang, H. Highly Stable and Sensitive Humidity Sensors Based on Quartz Crystal Microbalance Coated with Bacterial Cellulose Membrane. *Sens. Actuators, B* **2011**, *159* (1), 301−306.
(262) Alassi, A.; Benammar, M.; Brett, D. Quartz Crystal Microbalance Electronic Interfacing Systems: A Review. *Sensors* **2017**, *17* (12), 2799.
(263) Jha, S. N. Biosensor. In *Rapid Detection of Food Adulterants and Contaminants*; Elsevier: San Diego, 2016; pp 125−145. DOI: 10.1016/B978-0-12-420084-5.00005-6.
(264) Plácido, A.; Amaral, J. S.; Costa, J.; Fernandes, T. J. R. Novel Strategies for Genetically Modified Organism Detection. In *Genetically Modified Organis in Food - Production, Safety, Regulation and Public Health*, Watson, R. R., Preedy, V. R., Eds.; Elsevier: San Diego, 2016; Chapter 12, pp 119−131. DOI: 10.1016/B978-0-12-802259-7.00012-9.
(265) Vashist, S. K.; Vashist, P. Recent Advances in Quartz Crystal Microbalance-Based Sensors. *J. Sens.* **2011**, *2011*, 571405.
(266) Yao, Y.; Huang, X.-h.; Zhang, B.-y.; Zhang, Z.; Hou, D.; Zhou, Z.-k. Facile Fabrication of High Sensitivity Cellulose Nanocrystals Based QCM Humidity Sensors with Asymmetric Electrode Structure. *Sens. Actuators, B* **2020**, *302*, 127192.
(267) Hosseini, M. S.; Iraji zad, A.; Vossoughi, M.; Kalantarian, A. Development of a Quartz Crystal Microbalance Biodetector Based on Cellulose Nanofibrils (CNFs) for Glycine. *J. Mater. Sci.: Mater. Electron.* **2020**, *31* (20), 17451−17460.
(268) Hu, W.; Chen, S.; Liu, L.; Ding, B.; Wang, H. Formaldehyde Sensors Based on Nanofibrous Polyethyleneimine/Bacterial Cellulose Membranes Coated Quartz Crystal Microbalance. *Sens. Actuators, B* **2011**, *157* (2), 554−559.
(269) Wang, X.; Ding, B.; Sun, M.; Yu, J.; Sun, G. Nanofibrous Polyethyleneimine Membranes as Sensitive Coatings for Quartz Crystal Microbalance-Based Formaldehyde Sensors. *Sens. Actuators, B* **2010**, *144* (1), 11−17.
(270) Zhang, C.; Wang, X.; Lin, J.; Ding, B.; Yu, J.; Pan, N. Nanoporous Polystyrene Fibers Functionalized by Polyethyleneimine for Enhanced Formaldehyde Sensing. *Sens. Actuators, B* **2011**, *152* (2), 316−323.

https://doi.org/10.1021/acssensors.1c00473
ACS Sens. 2021, 6, 2473−2496